2010

Interaction of a translating tornado with a low-rise builsing

Hephzibah Thampi
Iowa State University

Interaction of a translating tornado with a low-rise building

by

Hephzibah Thampi

A thesis submitted to the graduate faculty

in partial fulfillment of the requirements for the degree of

MASTER OF SCIENCE

Major: Engineering Mechanics

Program of Study Committee:
Partha P. Sarkar, Co-Major Professor
Vinay Dayal, Co-Major Professor
Fouad S. Fanous

Iowa State University

Ames, Iowa

2010

TABLE OF CONTENTS

ACKNOWLEGDEMENTS

I would first like to thank God almighty without whom nothing would be possible. All glory and honor be to him alone.

I would like to express my sincere gratitude and appreciation for my major professor, Dr. Partha P. Sarkar, for his guidance and support during the past two years of study at Iowa State University. The past two years have been a special experience in my life. I would like to thank my co-major professor, Dr. Vinay Dayal for taking time to help me, especially in the structures laboratory and with finite element analysis. I also thank Dr. Fouad S. Fanous for being on my committee.

I would like to thank all the staff at the Department of Aerospace Engineering, specially Dee Pfeiffer and Gayle Fay, who helped me with all the paperwork and made my study here a memorable one. Sincere thanks to Bill Rickard Jim Wellman and the undergraduate students of the Department of Aerospace Engineering for their help in the laboratories. I would also like to thank the Department of Aerospace Engineering for providing me financial support in the form of a teaching assistantship for the major portion of my study here.

My deepest gratitude goes to my parents, the inspiration for my studies. Finally I thank my fiancé, sister, brother-in-law and friends for their prayers and support to help me complete my master's program successfully.

ABSTRACT

Nearly 1000 tornados are reported annually in the US. The annual damage caused by tornados can exceed one billion dollars. Of the damage caused, the most common and severely damaged structures are the conventional low-rise timber buildings which account for most of the residential buildings in the 'tornado alley'; the central region of the country, where most tornados occur. Little research has been done to study the effects of tornados on low-rise buildings. To predict the behavior of a conventional low-rise timber building under a translating tornado, it is necessary to capture its interaction with the tornado. This work focuses on studying the interaction of a tornado with a low-rise building.

In the first part of the work, a methodology was developed to predict the load time histories experienced by a low-rise building under a translating tornado using the existing load coefficients of the building in straight line winds. The effects of tornado-building interaction and sudden pressure drop or suction acting on the outer surfaces of the building, due to the tornado vortex, were preserved in the methodology. For design and analysis of buildings it is very often necessary to obtain the load time histories in a tornado. The relative positions of the building and tornado in general are arbitrary. It would be impossible to experimentally determine the loads on the building for all eventualities. It would also be very expensive to even try to undertake such a study. The methodology shows that it is sufficient to predict the load time histories of a building with respect to any arbitrarily located tornado. The knowledge of tornado induced load time histories for a few building-tornado combinations is all that is needed. A gable-roofed building model with a square plan, geometrically scaled to 1:100, and a tornado of swirl ratio 1.14 were used for this study.

In the second part of this work, the interaction of a tornado with a one-story gable-roofed timber building (with a rectangular plan) was studied. The methodology presented here predicted the successive stages of structural damage caused to the building by a translating tornado as a result of its interaction with the building components. The dynamic effects of changing internal and external pressures on the building were taken into account, as the tornado translated past the building and inflicted damage. A partially damaged one-story building, located within the damage path of the Parkersburg tornado (May 25, 2008), was

chosen for analysis using Finite Elements (FE). This tornado was rated EF5 by the National Weather Service. The observed damage was compared to that predicted in this study. The methodology described here enables accurate damage prediction and failure of a low-rise building from a tornado that will improve its component design and construction. Conversely, it also helps in assessing the intensity of a tornado from the observed damage state of the building.

CHAPTER 1

GENERAL INTRODUCTION AND BACKGROUND

1.1 INTRODUCTION

Tornados are strong atmospheric vortices that are products of well-organized conditions very favorable for their formation. The science of these giant atmospheric vortices is very complex and is still being studied (Kuo, 1966, 1971; Church, 1979; Fiedler, 1993). Tornados occur in many parts of the world, but are found to occur most frequently in the United States. They are concentrated in what is called the 'tornado alley', located in the central region of the country. There are thousands of tornados reported annually in the US, causing many fatalities and injuries. Though the annual damage caused by tornados exceeds one billion dollars, the study of damage prediction and its mitigation has only been an emerging topic in the field of wind engineering. Very often the most significant damage is caused to conventional low-rise, light-frame constructions. To study their damage prediction and mitigation, a good knowledge of the interaction of a translating tornado with the structure is required. This is a complex multi-physics problem but little to no studies exists so far. According to the current design codes, low-rise buildings in the tornado alley are built to withstand only up to 90 mph of straight-line winds, while 90% of the reported tornados generate anywhere from 40 to 157 mph. At the same time, these codes are based on studying the effects of straight line winds and not on tornado type winds on buildings, especially on low-rise, wood framed buildings which make up the majority of structures in the U.S. For the design of low-rise buildings under tornadic wind loads, it is essential to know the force time histories and the peak forces the building sees. Therefore, this work aims to address these problems.

1.2 MOTIVATION AND BACKGROUND FOR CURRENT RESEARCH

A few Studies have been performed in the past on the static and dynamic responses of structures in tornados. Wen (1975), Wen and Ang (1975) and Savory et al. (2001) performed

dynamic analyses of structures with a mathematically modeled tornado given by Kuo (1971). This model presented a three dimensional flow in the boundary-layer of the tornado-like vortex where the tangential, radial and vertical wind velocity profiles as functions of radial distance and height were obtained. The wind velocity profiles were used to calculate the time histories of the force-coefficients for the structure in the translating tornado. Dutta et al. (2002) studied the dynamic response of structures subjected to tornado loads by Finite Element (FE) method. He used an analytical model of a tornado suggested by Mehta et al. (1976). Sparks (1988) performed detailed static analyses of extreme wind loads on single storied wood framed houses. Jischke and Light (1983) used a slightly modified Ward (1972) tornado simulator to obtain force values of small building models with pressure measurement. Chang (1971) experimentally found the tornadic forces on a building with a basic tornado simulator. All of these analyses used either a mathematical/analytical model of a tornado or a simplified laboratory simulator which generated at best an approximate wind field in a tornado and therefore carried inherent limitations in the complex dynamic fluid-structure interaction between the tornado and the structure.

For the design and analyses of buildings under tornadic wind loads, it is often essential to know the time histories of the loads experienced by the building. As of today, the analytical models used to generate the time histories assume that the presence of the building does not affect the tornado wind field, i.e., tornado-building interaction is not considered. The effect of sudden suction experienced by the outer surfaces of the building, due to the tornado vortex is also neglected in most cases.
To overcome these shortcomings, for the design or analysis of even a simple low-rise building under tornadic loads, it is required to perform repeated tests in tornado simulators which can be expensive and time consuming, not considering the fact that there are only a limited number of facilities in the world (3 at present).

Another shortcoming of the past analyses performed to predict damage in buildings under tornadic wind loads was that the damage prediction was not performed to capture the failure of the structure in stages. The dynamic effects of constantly changing internal pressure and the wind flow's interaction with the structure must be accounted at different stages of failure to capture the true behavior of the structure and match its observed damaged state as seen on-

site in a damage survey. It is critical that the structural damage prediction of the structure be performed more accurately, as this knowledge helps to assess the intensity of the tornado that caused the damage, from the observed damage state of the building.

In view of these shortcomings, the following research tasks were proposed.

1. For the design and analyses of low-rise buildings under tornadic wind loads, it is essential to know the load time histories and the peak forces the building is subjected to. To eliminate the need for repeated tests in tornado simulators, develop and validate a methodology to compute the time histories of the mean load-coefficients for a low-rise building in a translating tornado, using the existing mean load-coefficients of the building in straight line winds, while preserving the effects of tornado-building interaction and sudden pressure drop or suction acting on the outer surfaces of the building, due to the tornado vortex.

2. Predict the damage of a conventional low-rise timber building in a translating tornado using FE method. Use a methodology that predicts the successive stages of structural damage caused to the building by a translating tornado as a result of its interaction with the building components.

3. Take into account the dynamic effects of constantly changing internal and external pressures on walls and roofs that occur as a result of partial or total loss of cladding, increase in stiffness due to the presence of internal walls, decrease of stiffness as a result of wall openings and deteriorating structural components during the storm.

4. Improve the accuracy of assessing the intensity of a tornado from the observed damage state of the building.

1.3 THESIS ORGANIZATION

The dissertation is written in the format of “Thesis Containing Journal Papers”. The dissertation includes contents modified from two manuscripts, out of which the second one (chapter 3) has been submitted for review to the Journal of Wind Engineering and Industrial Aerodynamics and the first (chapter 2) will be submitted to the International Journal of Wind and Structures. In addition, a general introduction chapter appears at the beginning and a conclusion and recommendations chapter is included at the end of the dissertation. An

appendix is added to the second manuscript (chapter 3) and contains figures that are referred to in chapter 3. All numerical simulations reported in this dissertation were conducted using MATLAB and ANSYS software.

The first journal paper describes a methodology developed to compute the time histories of the force-coefficients for a low-rise building in a translating tornado, from the existing mean force-coefficients of the same building in straight line winds, while preserving the effects of tornado-building interaction and sudden pressure drop or suction acting on the outer surfaces of the building, due to the tornado vortex. It also shows that it is possible to predict the time histories of the load-coefficients of a building located at any position with respect to (w.r.t.) the translating tornado, from the time histories of the load-coefficients of the same building at a given position w.r.t. the translating tornado, for few building-orientations. The methodology eliminates the need for repeated tests to obtain load-coefficients for design and analysis purposes. For this study, a tornado of swirl ratio S=1.14, was consistently maintained. The swirl ratio S is given by Eq.1.

$$S = \frac{r_1 \Gamma}{2Qh} \tag{1}$$

Where, r_1 is the radius of the domain of the tornado vortex, Γ is the circulation, Q is the volume flow rate per unit axial length and h is the inflow height.

The experimental data representing the wind velocity profiles in a tornado (Haan et al., 2008), the force-coefficients of a low-rise building in a translating tornado (Haan et al., 2010) obtained from the ISU's Tornado/Microburst Simulator (Haan et al., 2008) and the force-coefficients of the same low-rise building in straight line winds (measured in the Aerodynamics/Atmospheric Boundary Layer Wind and Gust Tunnel) were used to develop this methodology. The computed time histories were then validated experimentally in the ISU's Tornado/Microburst Simulator.

The second journal paper predicts the damage of a conventional low-rise timber building in a translating tornado using FE method. A partially damaged one-story building, located within the damage path of the Parkersburg EF5 tornado (May 25, 2008), was chosen for analysis using FE and comparison of observed damage to those predicted in this study. The Enhanced Fujita (EF) scale is one that rates the intensity of a tornado based on the observed

damage caused by it as seen on the damage site. The 3-second gust wind speed ranges of the EF scale is given below in Table 1.

EF scale	**3-sec gust wind speed mph (m/s)**
EF0	65-85 (29-38)
EF1	86-110 (38-49)
EF2	111-135 (49-60)
EF3	136-165 (60-73)
EF4	166-200(74-89)
EF5	>200 (>89)

Table 1. EF scale wind speed ranges

Experiments were performed to obtain the pressure data on a geometrically scaled model (1:75) of the building placed in the ISU's Tornado/Microburst Simulator. The parameters used to control tornado characteristics in the simulator were set to match the EF5 tornado as seen in Parkersburg. The pressure data was applied on a finite element model of the building and the failure modes of the structural components were identified at different stages. The experimental simulations were repeated with the partially damaged model as predicted by the FE analysis to assess the change in loading and then followed by subsequent FE analysis with the updated data. This sequence was repeated to replicate the observed damage of the example building. Strength tests of different nail connections were performed to find the load-displacement curves for different nail connections to better represent the behavior of the nail in the FE model. The final damage state of the building as predicted from the analysis was compared to that observed on the site and they matched well. The same analysis was repeated with tornados of intensities EF4 and EF3 to improve the assessment of the intensity of a tornado from the observed damage state.

CHAPTER 2

COMPUTATION OF TIME HISTORIES OF MEAN FORCE-COEFFICIENTS FOR A LOW-RISE BUILDING IN A TRANSLATING TORNADO, USING STRAIGHT LINE WIND DATA

Modified from a paper to be submitted to the journal of Wind and Structures

Hephzibah Thampi[a,b], Partha P. Sarkar[a,*], Vinay Dayal[a]

[a]Graduate student, Professor and Associate Professor respectively, Department of Aerospace Engineering, Iowa State University
[b]Primary author and researcher
[*]Corresponding author

ABSTRACT: The building codes to date specify design force-coefficients for straight line winds alone. From studies and experiments performed with the ISU's Tornado/Microburst Simulator, it has been found that these force-coefficients do not suffice in tornadic winds. For the design of low-rise buildings under tornadic wind loads, it is essential to know the force time histories and the peak forces the building is subjected to. To eliminate the need for repeated experimentation in well-equipped laboratories, a methodology was developed and validated to compute the time histories of the mean force-coefficients for a low-rise building in a translating tornado, using the existing mean force-coefficients of the building in straight line winds. This methodology preserves the effects of tornado-building interaction. This paper also describes the analytical model used to generate the mean wind velocity time–histories that cause dynamic wind-loading on the low-rise building in the translating tornado.

Keywords: time histories of mean force-coefficients; low-rise building; translating tornado; straight line wind.

1. INTRODUCTION

The building codes to date specify design force-coefficients for straight line winds alone. From studies and experiments performed with the ISU's Tornado/Microburst Simulator, it has been found that these force-coefficients do not suffice in tornadic winds (Sengupta et al.,

2008). For the design of buildings under tornadic wind loads, it is essential to know the load time histories and the peak loads the building experiences. At present, to obtain these loads, it is required to perform repeated testing in a tornado simulator that can be expensive, time consuming in addition to the fact that there are many boundary layer wind tunnels but only three tornado simulators in the world. To eliminate the need for such tests for the design of simple low-rise buildings, it was conceived that a methodology should be developed to compute the time histories of load coefficients for a low-rise building subjected to a translating tornado, from the existing mean load-coefficients of the building in straight-line atmospheric boundary layer (ABL) winds.

Efforts have been made in the past to simplify the model of a tornado so that the static and dynamic analyses of a structure subjected to tornadic wind loads could be performed. Wen (1975), Wen and Ang (1975) and Savory et al. (2001) performed dynamic analyses of structures with a theoretically modeled tornado given by Kuo (1971). The model presented a three dimensional flow in the boundary-layer of the tornado-like vortex where the tangential, radial and vertical wind velocity profiles as functions of radial distance and height were obtained. The wind velocity profiles were used to calculate the time histories of the force-coefficients for the structure in the translating tornado. Dutta et al. (2002) studied the dynamic response of structures subjected to an analytical model of a tornado suggested by Mehta et al. (1976). In all these studies, it was assumed that the presence of the building does not affect the tornado wind field, i.e., tornado-building interaction was not considered. Chang (1971) experimentally found the tornadic forces on a building with a basic tornado simulator. He stated that during the transient passage of the tornado by the building surface, the dynamic interaction is complex and stochastic in nature and hence the ensemble average of forces should be used for the study. The effects of wind-structure interaction cannot be neglected as they contribute heavily to the dynamic response of the structure. In addition to the above stated, most of the studies neglected the effect of sudden pressure deficit or suction on outer building surfaces during the passing of the tornado.

In this paper, a simple methodology is presented to compute the time histories of the mean force-coefficients for a low-rise building in a translating tornado from the existing mean force-coefficients of the same building in straight line ABL winds. The same methodology

can be extended to construct time histories of cladding pressures and moments on a building. This work shows that it is possible to predict the time histories of the load-coefficients of a building located at any position with respect to (w.r.t.) the translating tornado, from the time histories of the load-coefficients of the same building at a given position w.r.t. the translating tornado, for various building-orientations. This becomes useful when one requires the time histories of the load-coefficients at a given position for a given building-orientation but has the time histories for another position w.r.t. the translating tornado, for a few building-orientations, and wants to avoid repeated tests in a tornado simulator. To validate this methodology, the experimental data representing the wind velocity profiles in a tornado (Haan et al., 2008), the force-coefficients of a low-rise building in a translating tornado (Haan et al., 2010) measured in the ISU's Tornado/Microburst Simulator (Haan et al., 2008), the ground-plane static pressure profiles under a stationary tornado (Haan et al., 2010) also obtained from the ISU's Tornado/Microburst Simulator and the force-coefficients of the same low-rise building in straight line winds (measured in the Aerodynamics/Atmospheric Boundary Layer Wind and Gust Tunnel) were used. The ISU's Tornado/Microburst Simulator is large enough to accommodate models of structures of reasonable scale, comparable with that of the generated tornado and therefore simulates wind fields that closely match those of real tornados. Hence, the methodology used here preserves the tornado-building interaction, as will be shown in the following sections.

2. METHODOLOGY

2.1 Prediction of tornadic wind velocity time histories

To obtain the time histories of the mean force-coefficients, it is necessary to know the time histories of the tornadic wind velocity experienced at the building's location. A model was constructed to obtain the same, as described here. A tornado with 'Vane 5' settings (Haan et al., 2008) was consistently used for this study. The 'Vane 5' setting refers to a specific 'vane angle' set in the tornado simulator to generate a tornado vortex of a specific size (r_c=0.53 m), velocity ($V_{\theta max}$=9.7 m/s) and swirl ratio (S=1.14).

This methodology as outlined here can be adopted for tornados with other swirl ratios. The tornado case mentioned here was simulated on a smooth ground plane representing open

terrain conditions (Haan et al., 2010). Fig. 1 shows the normalized tangential velocity (V_θ/ $V_{\theta max}$) as a function of r/r_c at a height $z=0.52r_c$, where 'r' is the radial distance from the center of the tornado vortex and 'r_c' is the radius of the core of the tornado where the maximum tangential velocity $V_{\theta max}$ occurs.

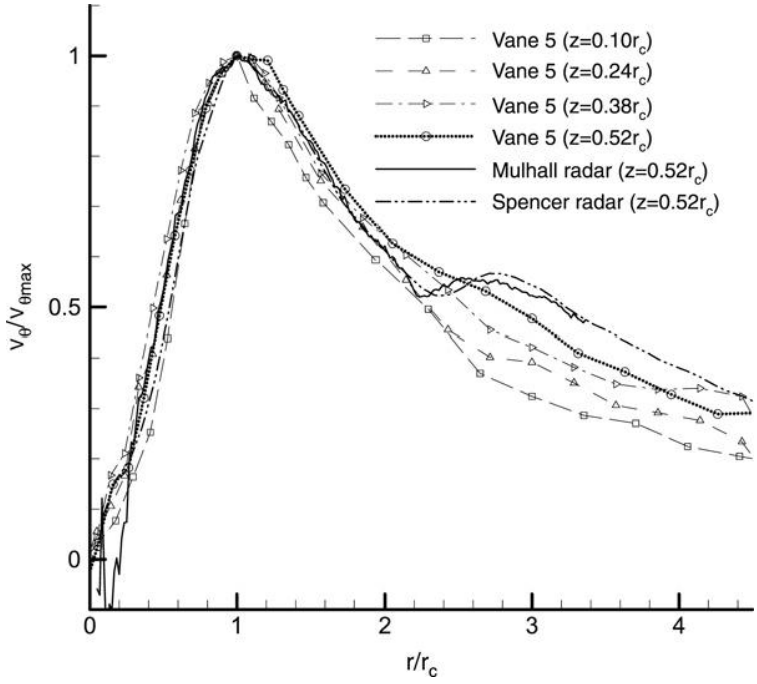

Fig. 1. Normalized tangential velocity profile for Vane 5 case at $z=0.52r_c$ (Haan et al., 2008)

It was assumed that this non-dimensional curve in Fig.1 was constant with height 'z' in the tornado, for locations not too close to the ground. The curve was split into three ranges of r for modeling: (1) from the center of the tornado-vortex to r_c, (2) the flat region from r_c to $1.224r_c$ and (3) $r \geq 1.224r_c$. A straight line given by Eqn.1 was fit to the first part, Eqn.2 represented the second part and the curve given by Eqn.3 was fit to the third part (Kuai et al., 2008).

$$\frac{V_\theta}{V_{\theta max}} \times \frac{r_c}{r} = 1, \quad 0 < r \leq r_c \tag{1}$$

$$V_\theta = V_{\theta max}, \quad r_c < r \leq 1.224r_c \tag{2}$$

$$\frac{V_\theta}{V_{\theta max}} \times \left(\frac{r}{r_c}\right)^{0.9} = 1.2, \quad r > 1.224r_c \tag{3}$$

The curve fitting exercise was repeated for the radial velocity. The normalized radial velocity profiles V_r/ $V_{\theta max}$, at four radial (r) distances $1r_c$, $2r_c$, $3r_c$ and $4r_c$, as a function of non-dimensional height z/r_c corresponding to 'Vane 5' settings (Haan et al., 2008) were chosen (Fig.2). Four different curves were fit to these profiles and are given by Eqn. 4. The constants C_1, C_2 and n in Eqn.3 as listed in Table.1 correspond to the four different radial velocity profiles.

$$\frac{V_r}{V_{\theta max(r)}} = C_1 \left(\frac{z}{r_c}\right)^n \left[1 - \text{erf}\left(c_2 \frac{z}{r_c}\right)\right] \quad (4)$$

Where, $V_{\theta max(r)}$ is the maximum tangential velocity at a radial distances r.

r/r_c	C_1	C_2	n
1	18.84	2.283	3.212
2	-2.345	3.738	1
3	-2.402	3.164	0.68652
4	-0.3958	0.1676	0.02002

Table 1. Constants for different radial velocity curves

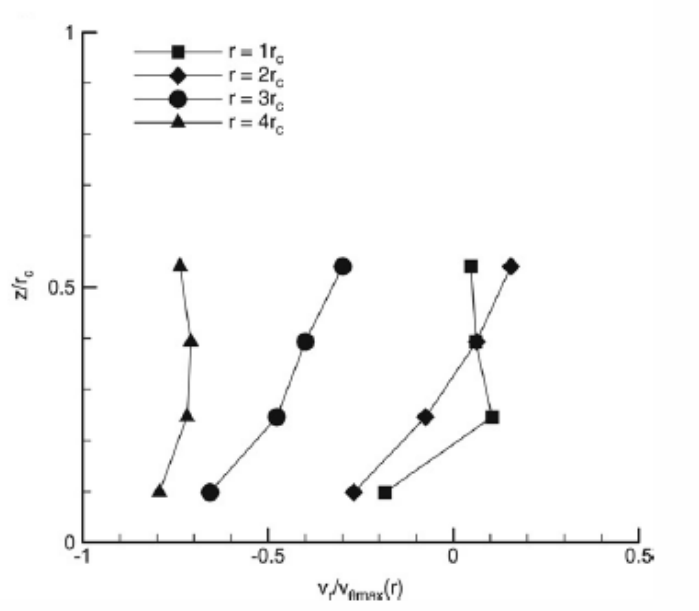

Fig. 2. Normalized radial velocity profiles at four radial distances for Vane 5 case (Haan et al., 2008)

The effect of vertical velocity was neglected in this study as it only 10% of the tangential velocity. Fig.3 shows the schematic diagram of the building-orientation w.r.t. the translating tornado. The building's major and minor axes were chosen as X and Y axes respectively, whose origin is located at the center of the building. The angle between the direction of the translating tornado and the X axis is'β' or building-orientation angle. *x* and *y* are distances from the center of the tornado to the building center in the building-axis system.

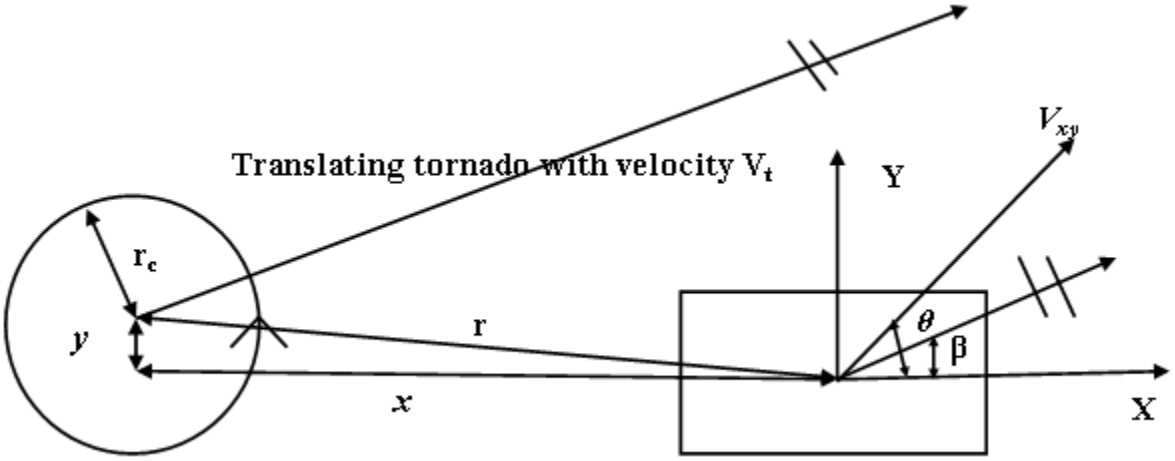

Fig. 3. Schematic diagram of building w.r.t. translating tornado

A computer program was written to compute the time/spatial-histories of V_x, V_y, V_{xy}, and θ, at the building origin, as the tornado translated by. V_x and V_y are the instantaneous wind velocity components in the X and Y directions respectively, seen at the origin. V_{xy} is the resultant instantaneous horizontal velocity making an angle θ with the X axis at the origin (Fig.3) which is also referred to as the instantaneous angle of attack (*AOA*). V_t is the translational velocity of the tornado. The inputs required for this program are $V_{\theta max}$, V_t, r_c, β, *z* (height at which the time histories for the horizontal velocities are required) and the initial values of *x* and *y* which can be considered as the location where the tornado touches down. The Eqns. (1-4) are first used to compute the starting values of V_x, V_y, V_{xy} and θ. A suitable time increment was used to define the new position of the translating tornado and iterations were performed to compute the time histories of these velocities at the building origin as the tornado moves past the building. As Eqns. (1-4) are used to compute the horizontal velocities, this program is valid for tornados having flow characteristics similar to the 'Vane

5' setting (Haan et al., 2008) only. The same methodology can be repeated for other types of tornados whose velocity profiles are measured or known, such as, Vane 1-4 settings in Haan et al. (2008). For ease of understanding, the velocities and force-coefficients are computed as a function of distance x or r, normalized w.r.t. core radius r_c (spatial-histories), instead of time. Fig. 4(a) shows the variation of V_x, V_y and V_{xy} ($=\sqrt{(V_x^2+V_y^2)}$) as a function of r/r_c of a typical EF5 tornado with $V_{\theta max}$= 89 m/s, V_t=16 m/s, r_c=130 m, β=0, z=3.2 m and initial distances x= -3.5r_c, y=0, where the tornado translates along the building axis X. Fig. 4(b) shows the spatial history of the instantaneous angle of attack θ.

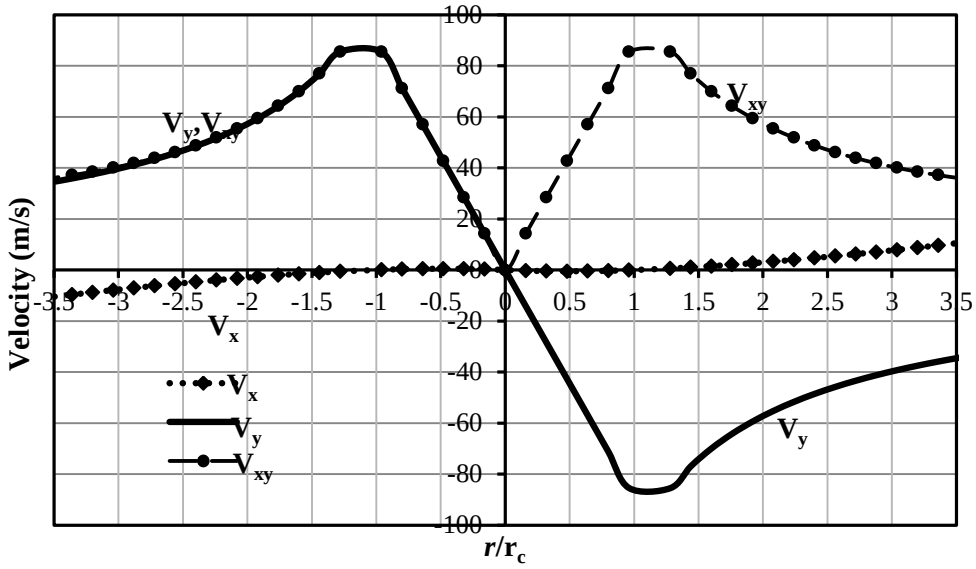

Fig. 4(a). Variation of V_x, V_y and V_{xy} as a function of r/r_c ($V_{\theta max}$= 89 m/s, V_t=16 m/s, r_c=130 m, β=0, z=3.2 m and initial distances x= -3.5r_c, y=0)

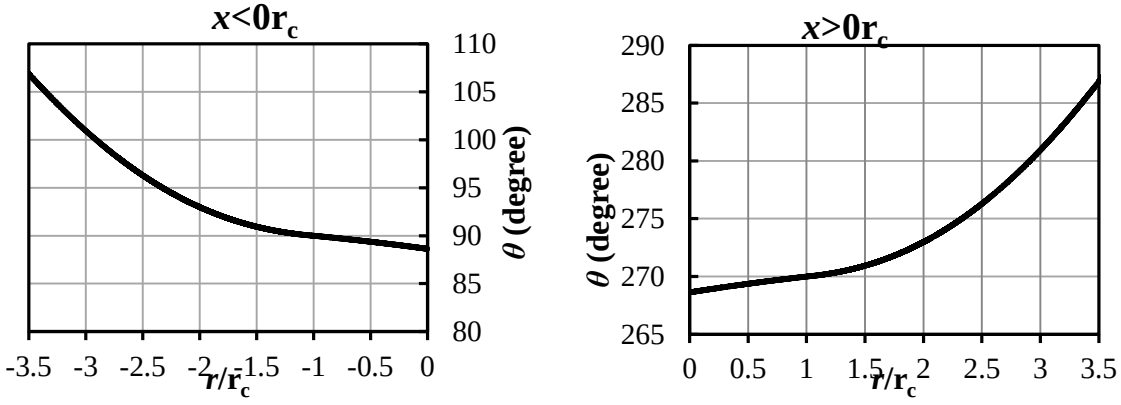

Fig. 4(b). Time history of instantaneous angle of attack θ

2.2 Prediction of time histories of force-coefficients

A one-storied gable-roofed building model with a roof angle of 35° and geometric scale of 1:100 and located on the centerline of a slow-moving laboratory tornado (y=0 at x=0 and V_t=0.15 m/s) was chosen for this study (Haan et al., 2010). The building model had a 91 mm×91 mm plan and an eave height of 36 mm. Time histories of the force-coefficients for this building corresponding to 'Vane 5' settings (Haan et al., 2008) as measured in the ISU's tornado simulator were used in the analysis.

The main objective of this study was to present a methodology to compute the time histories of the mean force-coefficients for a low-rise building in a translating tornado, from the existing mean force-coefficients of the building in straight-line ABL winds. Hence, it was decided to first prove that the mean force-coefficients C_{f_x} and C_{f_y} of a building in straight line winds (for different building-orientations β, where, β=θ in straight line winds) could be obtained from the time histories of the mean force-coefficients for the same building in a translating tornado. The time histories of the wind velocities computed using the computer program were required for this process. As the building is symmetric about the X and Y axes, it is aerodynamically similar in every quadrant. Therefore, it was sufficient to obtain its C_{f_x} and C_{f_y} for β varying from only 0° to 90° in straight line winds. As this process includes approximations, it is desirable to have multiple data sets. It was also found that many data sets were required to more accurately predict C_{f_x} and C_{f_y} as a function of β, over the wide range of β= 0° to 90° in straight line winds. Following this, the time/spatial histories of the force-coefficients of the building, located on the centerline of the translating tornado, for seven different building-orientation angles β= 0°, -15°,- 30°, -45°, -60°, -75°, and -90° were used. These force-coefficients were normalized w.r.t. $V_{\theta max}$ (9.7 m/s).

Fig. 5 shows the time-history of C_{f_x} and C_{f_y} for the building oriented at β= -90° on the centerline of the translating tornado as obtained experimentally. From studies performed to obtain velocity profiles for various swirl ratios (various vane angles) in the ISU tornado simulator, it was found that the magnitude of radial velocity was very small in comparison to the tangential velocity for tornado positions r= -4r_c to +4r_c. Therefore, for this case, the magnitude of V_y is negligible when compared to V_x, for tornado positions r (or y)= -4r_c to +4r_c. If the force experienced by the building in a translating tornado is a function of only the

instantaneous wind velocity (magnitude $|V_{xy}|$ and direction θ) at the position of the building, the value of C_{f_y} for r= -4r_c to +4r_c should be negligible when compared to the value of C_{f_x} in this range of r. Fig. 5 shows that the magnitude of C_{f_y} is not negligible and is comparable with C_{f_x} in this range. Hence, from observation and past literature (Chang, 1971) an assumption was made that the force experienced by a building in a translating tornado is an algebraically additive effect of both the instantaneous wind velocity at the position of the building and a suction caused by the translating vortex on the outer building surfaces. To convert the time histories of the force-coefficients of the seven building-orientation cases as functions of instantaneous horizontal velocity only, the following was performed.

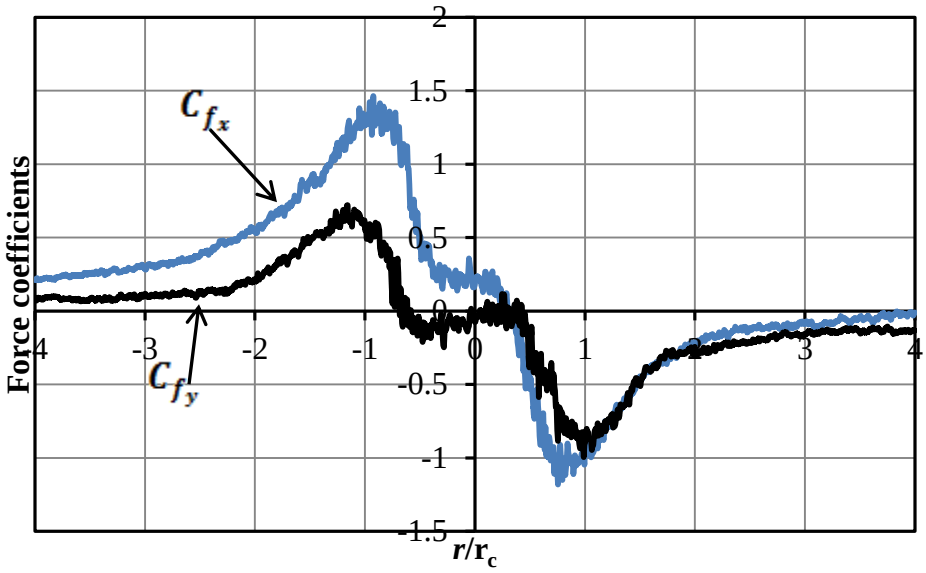

Fig. 5. C_{f_x} and C_{f_y} for the building oriented at (β=) -90° on the centerline of the translating tornado

The time histories of the variables V_x, V_y, V_{xy}, θ (at eave-height of the building), x, y and r, for the seven different building-orientation angles were obtained using the program developed to obtain wind velocity history in a translating tornado. Fig. 6 shows the ground plane static pressure (C_p) profile, measured under a stationary vortex (Haan et al., 2010), and normalized w.r.t. $V_{\theta max}$ (9.7 m/s) for the 'Vane 5' setting. An assumption was made that the external surfaces of the building experienced the same pressure drop (as shown in Fig. 6) under a translating tornado. Following this, the time histories of the coefficients C_p (Fig. 6), C_{f_x} and C_{f_y} are known as variations of r/r_c. To obtain the force-coefficients (C_{f_x} and C_{f_y}) as a

function of instantaneous velocity only, the effect of suction (C_p) on the surfaces of the building was subtracted from the corresponding values of $C_{f_x}$and C_{f_y}at every position of the tornado (corresponding to a discrete time points as calculated by the computer program). For example: for the building-orientation angle β= 0° and tornado's position *r*= -2r_c, the effect of suction on the left face of the building (–X plane) is C_p0.5ρ $V_{\theta max}{}^2$A, where, C_p is the suction pressure experienced by the left face of the building for a tornado's position *r*= -2r_c, 'ρ' is the density of air and 'A' is the projected area of the building on the X plane. The effect of suction on the right face of the building (+X plane) was similarly obtained, and these values were subtracted from the value of C_{f_x} at the tornado's position *r*= -2r_c.

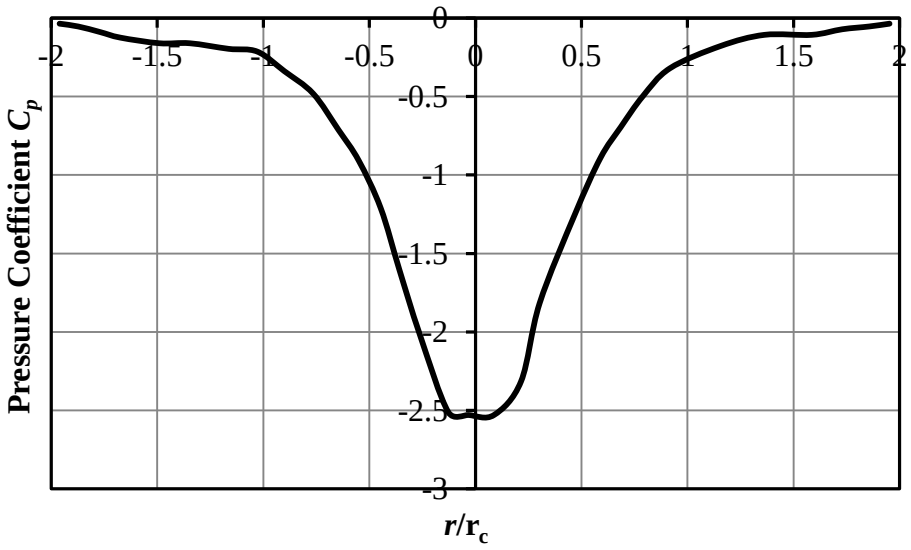

Fig. 6. Ground plane static pressure (C_p, suction) profile for 'Vane 5' setting (Haan et al., 2008)

The force-coefficients $C_{f_x}$and C_{f_y}corresponding to wind only for the seven different building-orientation cases obtained from this exercise as shown above were normalized w.r.t. the maximum tangential velocity $V_{\theta max}$. The wind velocity at the origin, in the translating tornado, continuously changes angles (θ) and horizontal velocity (V_{xy}). Therefore, unlike in a straight line wind, where the force-coefficients are functions of only θ *(AOA)*, these force-coefficients are functions of both θ *(AOA)* and magnitude of instantaneous horizontal velocity $|V_{xy}|$. For example: for the case β=0°, the values of $C_{f_x}$and $C_{f_y}$for the building at the tornado's position, *r*= -2r_c is a function of not only θ (formed by V_{xy} with the X axis at the

building's origin, at the tornado's position, r= -2r_c), but also is a function of $|V_{xy}|$ acting at the building's origin at the tornado's position r= -2r_c. To convert the spatial histories of these force-coefficients to functions of only the instantaneous angle of attack (θ), individual values of the time histories of these force-coefficients (C_{f_x} and C_{f_y}) were normalized w.r.t. the magnitudes of their corresponding instantaneous horizontal velocities $|V_{xy}|$. For example: for the case β=0° and r= -2r_c, the values of C_{f_x} and C_{f_y} at the tornado's position, r= -2r_c were normalized by 0.5ρ V_{xy}^2A, where, 'ρ' is the density of air, 'A' is an appropriate area used for normalization and V_{xy} is the instantaneous horizontal velocity acting at the building origin at an instantaneous θ when the tornado is located at the position r= -2r_c as calculated by the computer program.

The time histories of the force-coefficients (C_{f_x} and C_{f_y}) for the seven different cases of building-orientation angles became functions of only instantaneous angle of attack (θ°) like in straight line winds. As stated earlier, the building is aerodynamically similar in every quadrant and therefore the spatial-histories of these force-coefficient can be used to obtain force-coefficients (C_{f_x} and C_{f_y}) as a function of θ, from 0° to 90°, with 28 data sets (7×4), that sufficiently cover the entire range of θ. Fig. 7 shows the different values of θ (over a range of 0° to 90°), for the seven individual building-orientation cases (β) in the translating tornado. This represents the contribution of each case to the accurate prediction of force-coefficients as a function of θ for straight line winds.

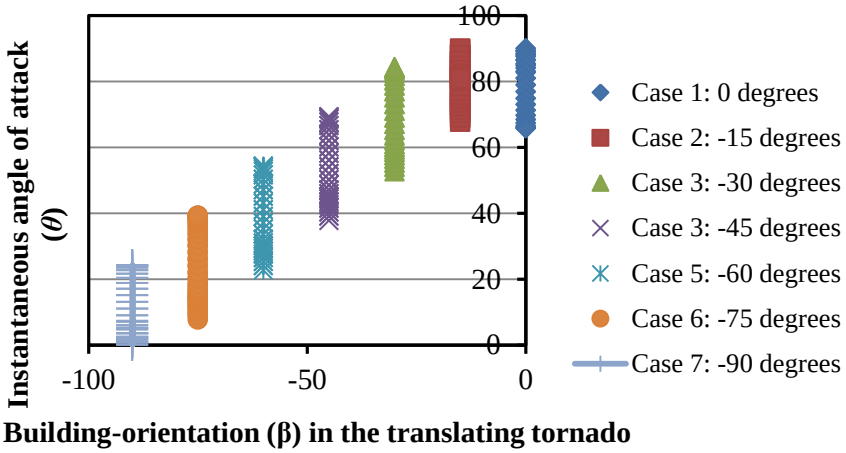

Fig. 7. θ (0° to 90°) for the 7 individual building-orientation cases (β) in the translating tornado. The tornado translates from r= -4r_c to r=+4r_c.

An experiment was set up to find the values of C_{f_x} and C_{f_y} for the same low-rise building in straight line winds for different building-orientations (β= 0°, 15°, 30°, 45°, 60°, 75° and 90°). This experiment was performed in the Aerodynamics/Atmospheric Boundary Layer Wind and Gust Tunnel (AABL) at ISU. An atmospheric boundary layer wind corresponding to open terrain atmospheric boundary-layer condition was generated by adding suitable roughness. The model was constructed as a single unit using a rapid prototyping technique and an aluminum rod was fixed at its center to connect through a hole in the ground plane of the wind tunnel to a force balance. The wind loads on this model were measured using this force balance (JR3 load cell Model 30E12A-I40) capable of measuring all three force and all three moment components. Force data were sampled at the rate of 500 Hz. The extracted values of the force-coefficients C_{f_x} and C_{f_y} as a function of θ in the tornado simulator for the seven building-orientation (β) cases in a translating tornado were compared with those measured in the AABL wind and gust tunnel as shown in Fig. 8 (a and b). Fig. 8(c) shows C_{f_x}, C_{f_y} and C_{f_z} for different building-orientations (β= 0°, 15°, 30°, 45°, 60°, 75° and 90°) as measured in the AABL wind and gust tunnel.

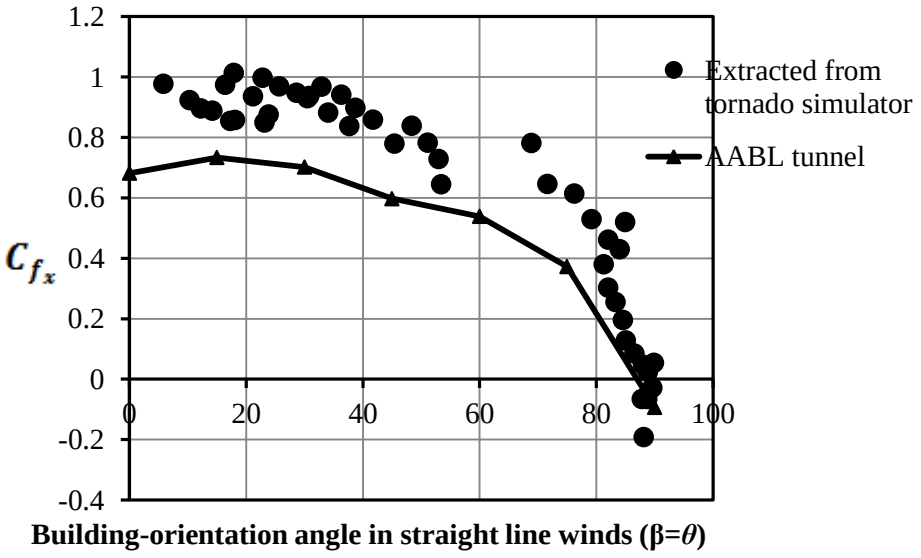

Fig. 8(a). Comparison of C_{f_x} extracted from the tornado simulator with experimental values measured in the AABL tunnel.

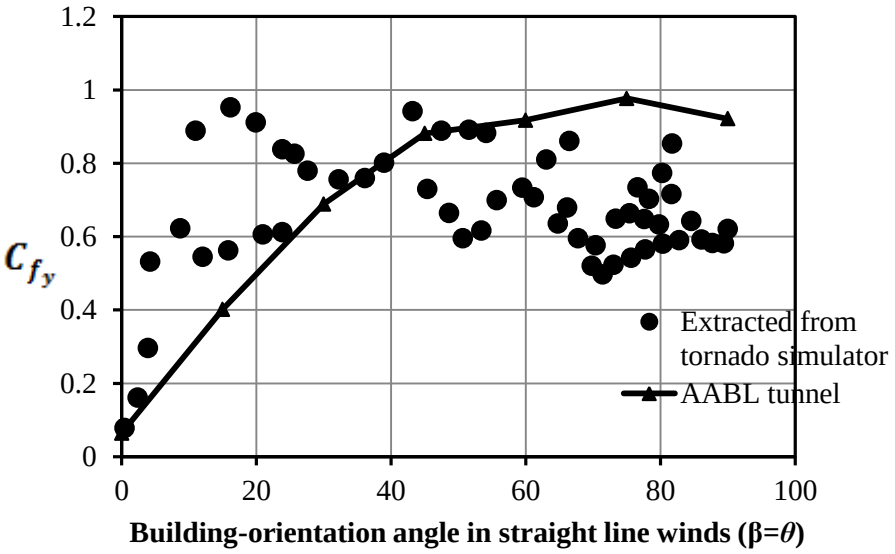

Fig. 8(b). Comparison of C_{f_y} extracted from the tornado simulator with experimental values measured in the AABL tunnel.

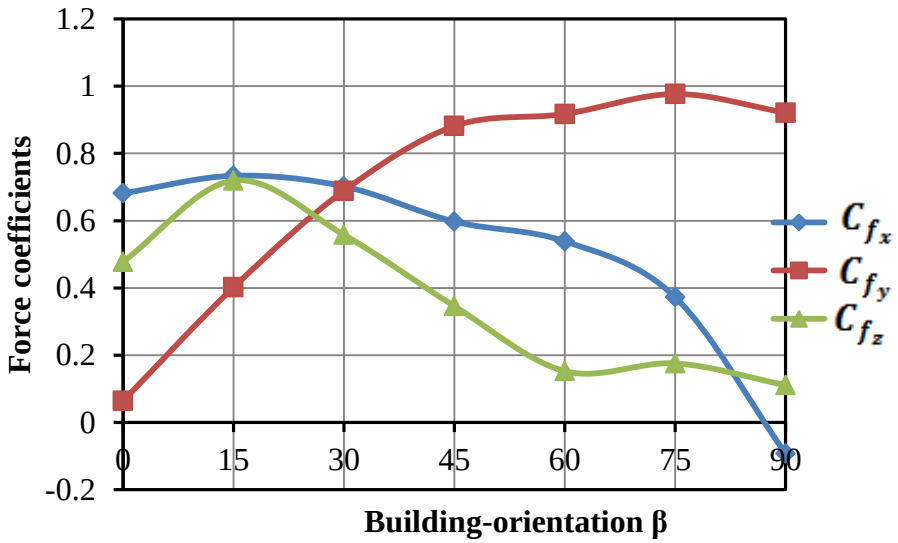

Fig. 8(c). Force coefficients C_{f_x}, C_{f_y} and C_{f_z} as a function of building-orientations (β) measured in the AABL tunnel

The extracted values of both C_{f_x} and C_{f_y} follow the general trend of those of straight line wind. Some of the sources of error could be that the effect of vertical velocity was

completely neglected and only an open terrain boundary-layer condition was assumed to exist in the tornado simulator.

As the methodology was proved right, the force-coefficients C_{f_x}, C_{f_y} and C_{f_z} of the building, as a function of building-orientation (β), obtained experimentally from the AABL wind and gust tunnel were used to obtain the time histories of the force-coefficients C_{f_x}, C_{f_y} and C_{f_z} for the same building situated anywhere in the translating tornado. This was done by using a program that simply reversed the computation process described in this section. An observation was made that as the length of the building was only $0.17r_c$, the contribution of the effect of suction due to the vortex on the outer surfaces of the walls, i.e., faces perpendicular to the ground plane, to the values of C_{f_x} and C_{f_y} would be small, if the pressure profile in Fig. 6 is used to obtain the effect of suction on the outer surfaces of the building perpendicular to the ground plane. This occurs as the surfaces that contribute to the values of C_{f_x} (walls on the +X and –X planes) and C_{f_y} (walls on the +Y and –Y planes) respectively are spaced at a distance of only $0.17r_c$ from each other and therefore, their combined effect on the force-coefficients as obtained from the pressure profile in Fig. 6 will be very small. But as discussed before, it is known that the effect of suction on the external surfaces of the building perpendicular to the ground plane is not negligible. Hence, it was concluded that the suggested method using the ground pressure profile (Fig. 6) to predict the contribution of suction on the external surfaces of the walls of the building to the values of C_{f_x} and C_{f_y} is insufficient and unrealistic. This could be another source of error for the scatter of the extracted data as seen in Fig. 8(a and b). Moreover, as the planes of the walls are perpendicular to the ground plane, the effect of suction due to the vortex on the walls could be different from a plane that is parallel to the ground (e.g. roof).

In an effort to model and capture the effect of suction on the outer surfaces of the building better, the time history of C_{f_y} for the building located on the centerline and orientated at β= -90° was chosen (Fig. 5). It is already known that the magnitude of the radial velocity (or V_y in this case) is negligible when compared to the tangential velocity (V_x in this case), for tornado positions r (or y)= $-4r_c$ to $+4r_c$. Therefore, the force (C_{f_y}) experienced by the building in the Y direction for these positions must be due to the suction on the outer surfaces of the

building (surfaces projected on the +Y and –Y planes respectively). The effect of suction does not show up in the values of C_{f_x} for this building-orientation case because the surfaces (walls on the +X and –X planes) that contribute to the value of C_{f_x} are always equidistant from the location of the translating tornado and therefore their suction effects completely nullify each other.

An assumption was made that the values (time history) of C_{f_y} for this building-orientation case were only due to the effect of suction on the outer surfaces on the +Y and –Y planes respectively, for tornado positions r= -4r_c to +4r_c. As these values (time history) were normalized w.r.t. the effective area that contributed to the force in the Y direction, they approximately equal the time history of the effective C_p experienced by the area of the building projected on a plane perpendicular to the radial distance r between the center of the building and the center of the translating tornado. Fig. 9 shows this effective profile of C_p that was used to replace the ground pressure profile (Fig. 6) and used to represent the contribution of the suction on the external surfaces of the building (perpendicular to the ground plane) to the time histories of $C_{f_x}$and C_{f_y}. For example: the contribution of suction on the external walls of the building for any building-orientation, to the horizontal force (F_{xy}) experienced by the building at r= -2r_c is C_p0.5ρ $V_{\theta max}{}^2$A, where, C_p is the effective pressure coefficient at the tornado's position r= -2r_c (from Fig. 9) and 'A' is the area of the building projected on a plane perpendicular to the radial direction at r= -2r_c. It will be proven that this model is a better representation of the effect of suction on the external surfaces of the walls (surfaces perpendicular to the ground plane). The ground pressure profile in Fig. 6 was still used to predict the contribution of the suction on the roof to C_{f_z}.

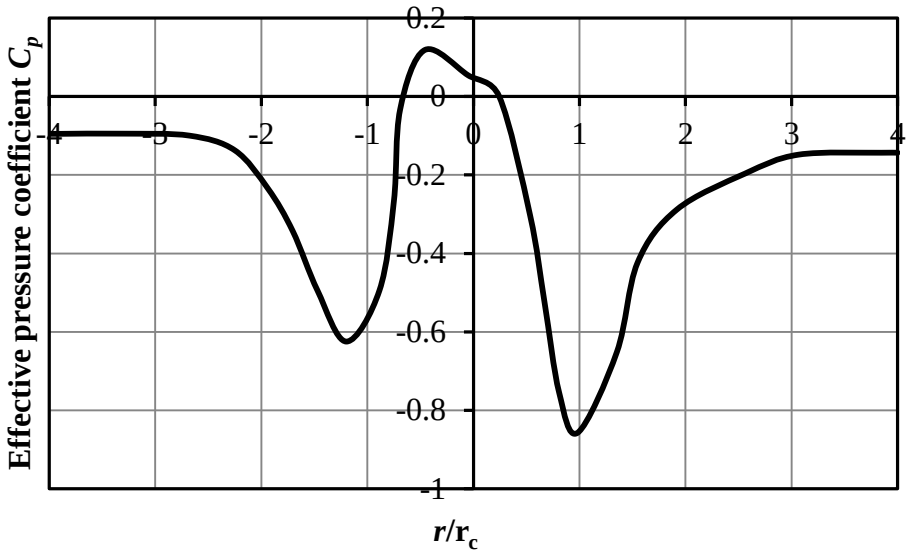

Fig. 9. Effective wall pressure profile (C_p, suction)

It can be seen that the time history of C_{f_y} in Fig. 5 is the same as the profile of effective C_p in Fig. 9. This is because the time history of C_{f_y} in Fig. 5 was used to obtain effective C_p in Fig. 9 as explained above. There is only a change in signs between these two curves and is attributed to the fact that C_{f_y} is the coefficient of force in the Y direction and it changes sign as the tornado passes over the building, while, effective C_p is the coefficient of effective suction (negative pressure) experienced by the outer surfaces of the building perpendicular to the ground plane, in the direction of instantaneous radial distance r as the tornado translates by. While obtaining effective C_p profile (Fig. 9) from the time history of C_{f_y} (Fig. 5) an assumption was made that the values (time history) of C_{f_y} were only due to the effect of suction on the outer surfaces on the +Y and –Y planes respectively, for tornado positions r= -4r_c to +4r_c and not due to radial velocity V_r. This is an approximation that was made to successfully model the effect of suction on surfaces perpendicular to the ground plane as explained. The positive values of effective C_p in the range of r= -1r_c to +1r_c (Fig. 9) can be attributed to this reason. The values of C_p in this range must go to zero as the surfaces on the +Y and –Y plane (surfaces that contribute to effective C_p) are equidistant from the center of the tornado when the tornado is right above the building (r=0). Moreover, it is well known that the outer surfaces of a building in a tornado are always under the influence of constant

suction (e.g. Fig. 6). Hence, the presence of effective positive pressure due to the vortex on the building's external surfaces (perpendicular to the ground plane, in the direction of radial distance r) for r= -1r_c to +1r_c (Fig. 9) is an approximation that cannot be avoided so that the effect of suction can be modeled better as explained before. It should be noted that the time history of C_{f_x} for a building's orientation β= 0° can also be used to obtain the profile of effective C_p experienced by the outer surfaces of the building perpendicular to the ground plane, in the direction of instantaneous radial distance r by repeating the same exercise performed to obtain C_p (Fig. 9) from C_{f_y} (Fig. 5). The building orientation case β= -90° was chosen instead, as the outer surfaces on the +Y and –Y plane respectively that contribute to the effect of suction in C_{f_y} are larger when compared to the outer surfaces on the +X and –X planes that would contribute to the effect of suction in C_{f_x} for the case with β= 0°. As the area used to normalize C_{f_y} is large, the error that might show up in effective in C_p is reduced.

It was expected that the computed time-history for C_{f_z} would be quite approximate as the effect of vertical velocity was neglected while computing the time histories of the wind velocities. This methodology is advantageous as it takes into account the changes in the tornado wind-field that occur due to the presence of the building, i.e., the force coefficients as a function of building-orientation (β) in straight line winds are used to calculate the time histories of the force coefficients in a translating tornado. The sudden effect of suction due to the tornado vortex on the outer surfaces of the building is also taken into account.

3. VALIDATION

The effect of vertical velocity was neglected for this study as the main objective was to present the methodology and validate it. It is well known that the vertical wind velocity in a tornado is not independent of the horizontal wind velocities. For positions both within the tornado-vortex core and above the boundary-layer, the time histories of the force-coefficients of the low-rise building in the translating tornado, resulting from computation using the methodology as described in the previous section, were expected to be quite approximate (Kuo, 1966, 1971; Wen, 1975; Wen and Ang, 1975). Hence, it is sufficient to validate the methodology for positions outside this region of doubt (e.g. y= -1.42r_c at x=0). The same

methodology can be repeated taking the effects of vertical velocity into account and more accurate results may be obtained.

To validate the methodology presented, the same gable-roofed low-rise building model as used before in experiments to obtain force-coefficients in the ISU's Tornado/Microburst Simulator and in the ISU's AABL wind tunnel, was placed at a position $y= -1.42r_c$ (at $x=0$) with building-orientation $\beta=0$ in the ISU's Tornado/Microburst Simulator. 'Vane 5' settings (S=1.14) were maintained and open terrain atmospheric boundary-layer conditions were assumed. Force coefficients were obtained for a quasi-steady tornado (Sengupta et al., 2008), for tornado positions starting at $x= -3.5r_c$ to $3.5r_c$ in steps of $0.5r_c$. It has already been shown (Sengupta et al., 2008) that the effect of translational velocity as low as 0.3 m/s in the laboratory is not significantly different from the quasi-steady case for larger distances of the tornado from the building, say $x \geq 2r_c$. They have also showed that the time histories of the force-coefficients in the translating tornado of speed 0.30 m/s were not shifted as much in position from the force-coefficients measured in the quasi-steady case as those in a translating tornado of speed 0.61 m/s, whose peak force-coefficients were shifted in position by nearly $1.0r_c$ from the quasi-steady case. The distance $x= -3.5r_c$ was chosen as the starting point to obtain force-coefficients in the quasi-steady tornado because the building started experiencing noticeable loads when the tornado reached this position. The force-coefficients obtained experimentally from the tornado simulator were compared against the spatial histories of the force-coefficients computed at $V_t=0.3$ m/s using the methodology proposed in this paper and are shown in Fig.10. As explained before, the spatial histories of the force-coefficients computed for the translating tornado (0.30 m/s) were expected to vary in magnitude (for positions close to $x=0$) and also slightly in position from the force-coefficients obtained experimentally for the quasi-steady tornado.

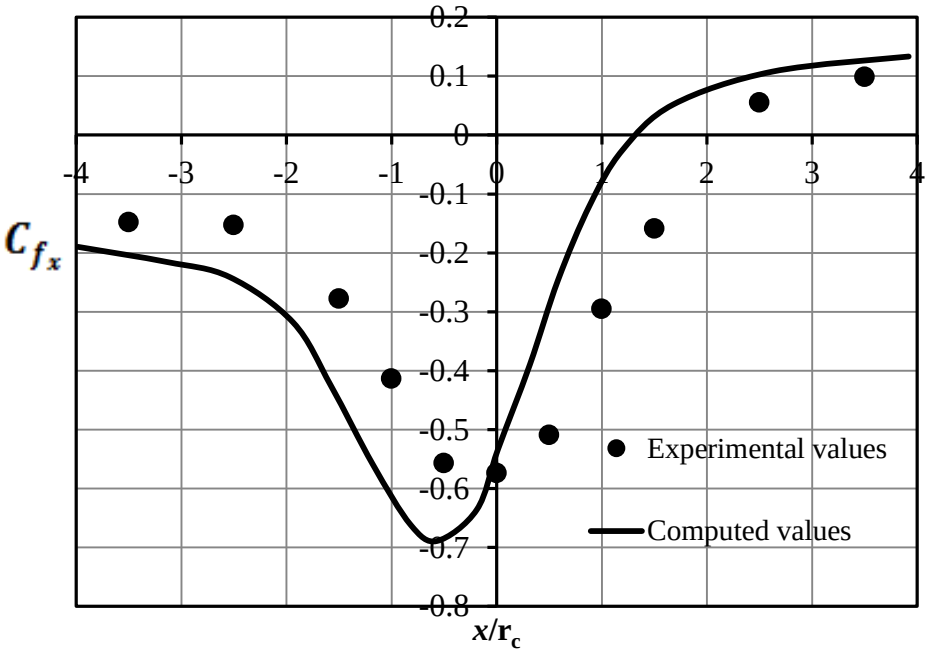

Fig. 10(a). C_{f_x}, a function of x/r_c, experimental vs. computed

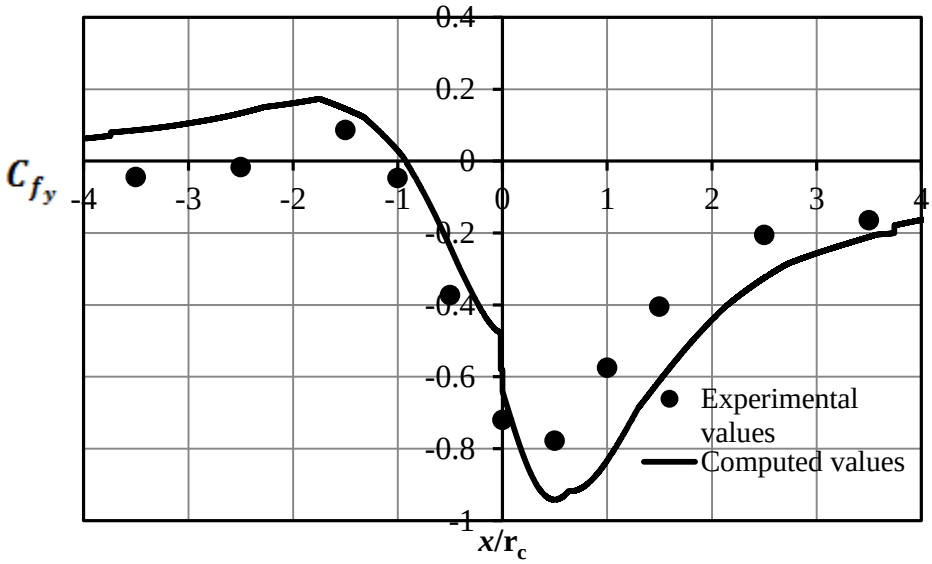

Fig. 10(b). C_{f_y}, a function of x/r_c, experimental vs. computed

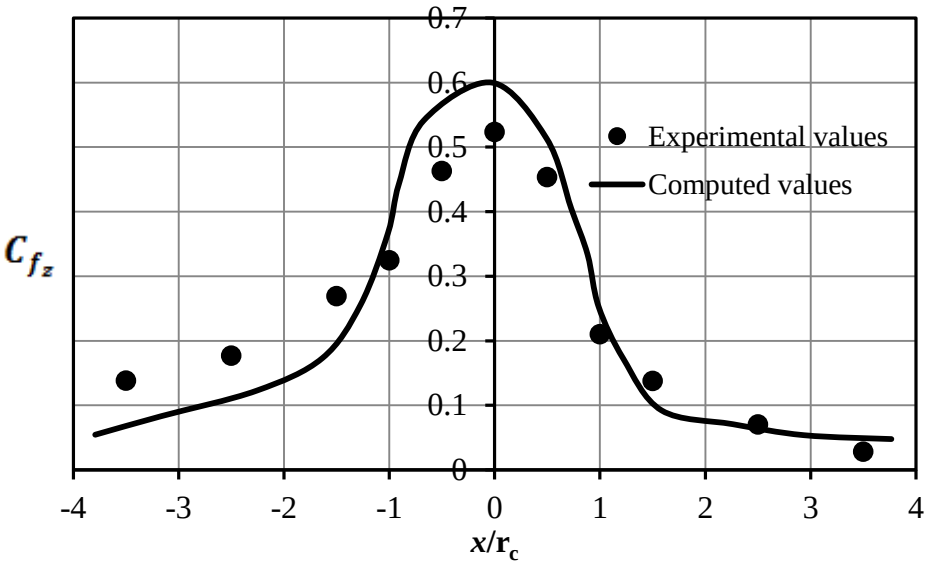

Fig. 10(c). C_{f_z}, a function of x/r_c, experimental vs. computed

The computed values of all the three force-coefficients C_{f_x}, C_{f_y} and C_{f_z} compare quite well with the experimental values. The peaks of the computed values are slightly higher than the experimental ones. This could be because the computed values are for a tornado of translating velocity 0.3 m/s and the experimental ones are for a quasi-steady tornado, as explained earlier in this section. In addition to this, the ground and wall pressure drop profiles used for predicting the force time histories as shown in Fig. 6 and Fig. 9 are due to a tornado translating at a velocity of 0.15 m/s, while the predicted force coefficients are being compared to those under a quasi-steady tornado. The slight shift in the trends of the computed time histories curves w.r.t. the experimental ones could also be attributed to the same causes. While predicting the effect of suction on the outer surfaces of the building perpendicular to the ground plane using C_p in Fig. 5 from C_{f_y} in Fig. 5, it was assumed that the profile of C_{f_y} was purely due to the effect of suction on the outer surfaces perpendicular to the ground plane. The contribution of the effect of radial velocity to C_{f_y} was neglected for tornado's positions r= -4r_c to +4r_c. This is an approximation that was made to successfully model the effect of suction as explained before. This may be another source of error for the time histories shown in Fig. 10. As the building is outside the radius of the core of the

tornado at all times, the values of C_{f_z} compare quite well too. On a whole, the results seem to compare well and thereby validate the proposed methodology.

4. CONCLUSION

An analytical model was developed to generate the mean wind velocity time histories that caused dynamic wind-loading on a low-rise building in a translating tornado. A methodology was developed to compute the time histories of the mean load-coefficients for the same low-rise building in the translating tornado, from the existing mean load-coefficients of the building in straight line winds, using the analytical model created to generate the mean wind velocity time histories. Results were validated by performing experiments in the ISU's Tornado/Microburst Simulator and the AABL wind tunnel at ISU. This methodology eliminates the need for repeated and cumbersome experimentation in tornado simulators that can be expensive, time consuming and inefficient for the design of a simple conventional low-rise building. It also is advantageous as it takes into account the changes in the tornado wind-field that occur due to the presence of the building and also the effect of sudden pressure drop or suction due to the vortex that is experienced by the outer surfaces of the building. The effects of vertical wind velocity were neglected for this paper. In future, methodology can be made more accurate by incorporating the effects of vertical wind velocity into it.

REFERENCES

Chang, C.C., 1971. Tornado wind effects on buildings and structures with laboratory simulation. Proceedings of the Third International Conference on Wind Effects on Buildings and Structures, Tokyo, 213–240.

Dutta, P.K., Ghosh, A.K., Agarwal, B.L., 2002. Dynamic response of structures subjected to tornado loads by FEM. Journal of Wind Engineering and Industrial Aerodynamics 10, 55-69.

Haan, F.L., Balaramudu, V.K., Sarkar, P.P., 2010. Tornado-induced wind loads on a low-rise building. American Society of Civil Engineers, Journal of the Structural Division 136, 106–116.

Haan, F.L., Sarkar, P.P., Gallus, W.A., 2008. Design, construction and performance of a large tornado simulator for wind engineering applications. Engineering Structures 30, 1146-1159.

Kuai, L. Haan, F.L., Gallus, W.A., Sarkar, P.P., 2008. CFD simulations of the flow field of a laboratory-simulated tornado for parameter sensitivity studies and comparison with field measurements. Wind and Structures 11, 75-96.

Kuo, H.L., 1966. On the dynamics of convective atmospheric vortices. Journal of Atmospheric Sciences 23, 25-42.

Kuo, H.L., 1971. Axisymmetric flows in the boundary layer of a maintained vortex. Journal of Atmospheric Sciences 28, 20-41.

Mehta, K.C., Mcdonald, J.R., Minor, J., 1976. Tornadic loads on structures. Proceedings of the Second USA–Japan Research Seminar on Wind Effects on Structures, Tokyo, Japan, 15–25.

Savory, E., Parke, G.A.R., Zeinoddini, M., Toy, N., Disney, P., 2001. Modeling of tornado and microburst-induced wind loading and failure of a lattice transmission tower. Engineering Structures 23, 365-375.

Sengupta, A., Haan, F.L., Sarkar, P.P., Balaramudu, V., 2008. Transient loads on buildings in microburst and tornado winds. Journal of Wind Engineering and Industrial Aerodynamics 96, 2173-2178.

Wen, Y.K., 1975. Dynamic Tornadic wind loads on tall buildings. American Society of Civil Engineers, Journal of the Structural Division 101, 169–185.

Wen, Y.K., Ang, A.H.S., 1975. Tornado risk and wind effects on structures. Proceedings of the Fourth International Conference on Wind Effects on Buildings, Heathrow, 63–74.

CHAPTER 3

FINITE ELEMENT ANALYSIS OF INTERACTION OF TORNADOS WITH A LOW-RISE TIMBER BUILDING

Modified from a paper submitted to the Journal of Wind Engineering and Industrial Aerodynamics

Hephzibah Thampi[a,b], VinayDayal[a], Partha P. Sarkar[a,*]

[a]Graduate student, Associate Professor and Professor respectively, Department of Aerospace Engineering, Iowa State University
[b]Primary author and researcher
[*]Corresponding author

ABSTRACT: This paper studies the interaction of a tornado with a one-story gable-roofed timber building. The methodology presented in this paper will predict the successive stages of structural damage caused to the building by a translating tornado as a result of its interaction with the building components. The dynamic effects of changing internal and external pressures on the building are taken into account, as the tornado translates by the building and inflicts damage. A partially damaged one-story building, located within the damage path of the Parkersburg EF5 tornado (May 25, 2008), was chosen for analysis using Finite Elements (FE) and comparison of observed damage to those predicted in this study. The methodology described here enables accurate damage prediction and failure of a low-rise building from a tornado that will improve its component design and construction. It also helps in assessing the intensity of a tornado from the observed damage state of the building.

Keywords: Gable-roofed timber building; dynamic pressure; tornado interaction; FE analysis; failure modes of structure; EF-scale assessment

1. INTRODUCTION

The annual damage caused by tornados on life and property can exceed one billion dollars and yet the study of damage prediction and its mitigation has only been an emerging topic in the field of wind engineering. The interaction of a translating tornado with conventional light-frame construction is a multi-physics problem but little to no studies exists so far. Dutta

et al. (2002) studied the dynamic response of structures subjected to tornado loads by Finite Element (FE) method. In this study, an analytical model of a tornado was used as suggested by Mehta et al. (1976). Sparks (1988) performed detailed static analyses of extreme wind loads on single storied wood framed houses. Wen (1975), Wen and Ang (1975) and Savory et al. (2001) performed dynamic analyses of structures with a mathematically modeled tornado. Chang (1971) experimentally found the tornadic forces on a building with a basic tornado simulator. Jischke and Light (1983) used a slightly modified Ward (1972) tornado simulator to obtain force values of small building models with pressure measurement. All of these analyses used either a mathematical/analytical model of a tornado or a simplified laboratory simulator which generated at best an approximate wind field in a tornado and therefore carried inherent errors in the complex fluid-structure interaction between the tornado and the structure. Therefore, it was necessary to have a physical tornado simulator that was large enough to accommodate models of structures of reasonable size and simulate wind field that closely matched those of the real tornados. The ISU's Tornado/Microburst Simulator (Haan et al., 2008) was used to serve this purpose. The other shortcoming of the past analyses was that the FE analysis was not performed to capture the failure of the structure in stages. The dynamic effects of constantly changing internal pressure and the wind flow's interaction with the structure must be accounted at different stages of failure to capture the true behavior of the structure and match its observed damaged state as seen on-site in a damage survey. This study aims at addressing these shortcomings so that structural damage prediction in a tornado can be done more accurately such that tornado wind speeds that caused these damages can be estimated more accurately from the observed damage state of the structure and mitigation measures can be devised to prevent or alleviate these damages in tornados of medium intensity. This study is similar to that of Kumar (2008) at ISU, except the effects of changes in internal and external pressures on walls and roofs that occur as a result of partial or total loss of cladding, increase in stiffness due to the presence of internal walls, decrease of stiffness as a result of wall openings and deteriorating structural components during the storm are included.

Experiments were performed to obtain the pressure data on a geometrically scaled model (1:75) of the building placed in the ISU's Tornado/Microburst Simulator. The pressure data

was applied on a finite element model of the building and the failure modes of the structural components were identified at different stages. The experimental simulations were repeated with the partially damaged model as predicted by the FE analysis to assess the change in loading and then followed by subsequent FE analysis with the updated data. This sequence was repeated to replicate the observed damage of the example building. Strength tests of different nail connections were performed to find the load-displacement curves for different nail connections to better represent the behavior of the nail in the FE model. This methodology will (a) enable accurate damage prediction and failure of a low-rise building from a tornado that will improve its component design and construction, (b) provide a better understanding of the influence of dynamically varying internal pressure on the building performance during a tornado, and (c) help in assessing the intensity of a tornado from the observed damage state of the building.

2. FULL SCALE BUILDING CHOSEN FOR ANALYSIS

Buildings located along the center-line of the tornado path are expected to see maximum damage including complete collapse. Hence, a partially-damaged building was chosen for analysis in this study so that its predicted damage state could be compared with that observed at the site. The building used in the analysis is not exactly same but similar to the one-story gable-roofed building that was partially damaged in the Parkersburg tornado (EF5) of May 25, 2008. The partially-damaged building that was chosen for comparison was located away from the center-line of the tornado path as observed during the post-damage survey (Sarkar and Kikitsu, 2008). Fig.1 shows the position of this example building with respect to the damage path of the tornado.

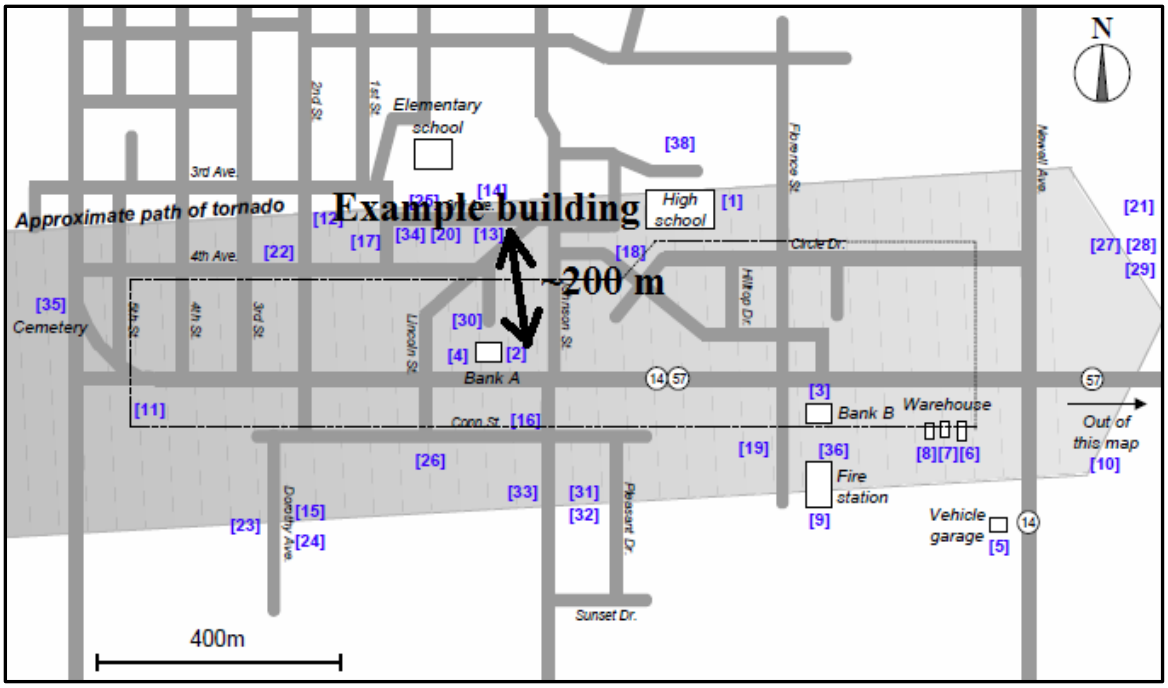

Fig. 1. Example building at Parkersburg w.r.t. damage path of tornado (Sarkar and Kikitsu, 2008)

The building used in the analysis is a one-story gable-roofed two-bedroom residential building with timber construction and a rectangular plan with dimensions 15m x 10m. It has an eave height of 3m and a roof slope of 16°. The structural design and detailing of this building was performed in accordance with the provisions of IBC (2006), APA (1997) and AF&PA (2001). It is to be noted that since the building was located at Parkersburg, Iowa, it was designed for Seismic Category B and Wind Exposure Category C. The design wind speed that was used was 40 m/s (90 mph), 3-sec gust, at 10 m elevation in an open terrain, as specified by the building code (IBC, 2006).

The building consisted of internal walls, windows and doors. Gable end trusses were provided at both the roof ends. The interior trusses were 2-web trusses of 10 m (32-feet) span, designed and retrofitted with wind bracing to withstand the basic design wind speed at that location. The wall studs were spaced 0.4 m (16 inches) on center and the roof trusses were spaced 0.6 m (24 inches) on center. At the intersection of two or more walls (corner), wall studs were placed at a distance of 0.1 m (4 inches) from the corner, in each wall, in addition to the wall studs spaced at 0.4 m on center. Studs of dimension 38 mm x 89 mm (2x4) were provided for walls, gable end trusses and purlins.

The sole and head plate consisted of 2-2x4 and the header consisted of 2 studs of dimension 38mm x 235mm (2x10) each. Studs of dimension 38mm x 184mm (2x8) were used for the ridge piece and top chords of the gable end trusses. Douglas –Fir was consistently used for all beams and studs. Fig.2 shows the plan of the building, used in the analysis.

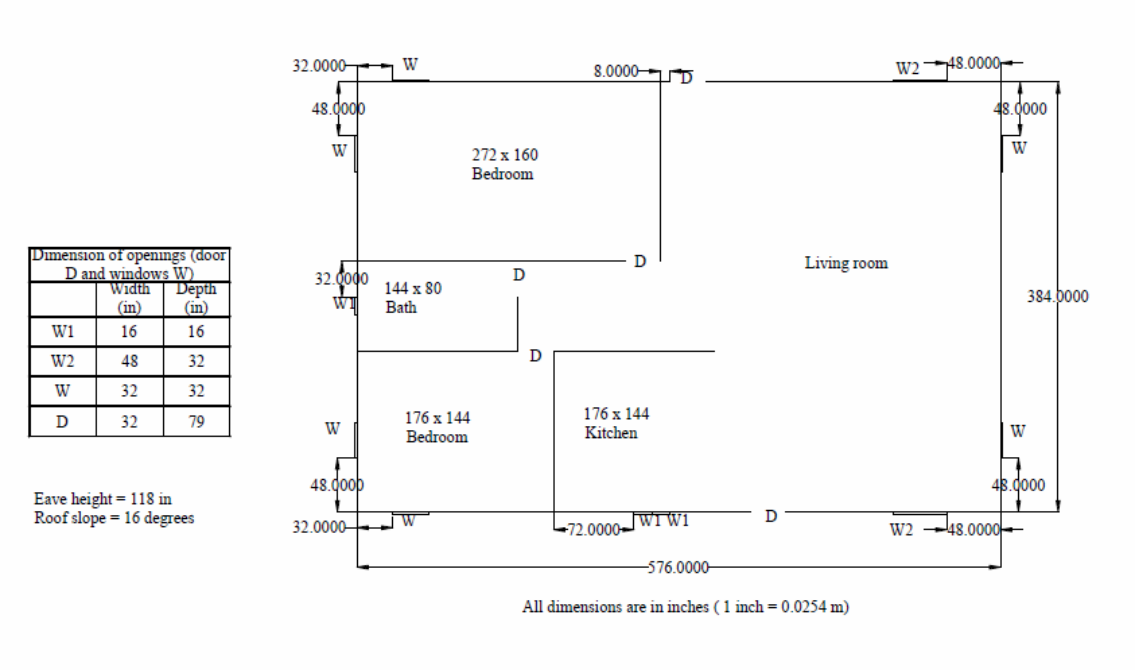

Fig. 2. Plan of building used in the analysis

Douglas Fir-Larch (structural I C-D) wood structural panels of thickness 0.0127m (0.5 inch) were used as sheathing. Standard 8d common nails (length 63.5 mm, diameter 3.327 mm) were used at less than 203 mm (8 inches) on center for the sheathing. Windows were modeled with the plexiglass of thickness 6mm (0.25 inch) and elastic modulus 3102.6 MPa (450 ksi) as taken from Matweb (2010). Wall studs were connected to the sole and the head plate by 2-16d common face nails (length 88.9 mm, diameter 4.11mm). In addition to these connectors for the wall studs at corners and openings (windows and doors), special uplift connectors were used. Blocking in between trusses to the head plates were connected by 3-8d common toe nails per blocking to enable transfer of lateral shear forces in between trusses and also in between roof and wall diaphragms. The trusses were connected at the corners to the head plate by a minimum of 4-8d common toenails per corner in addition to special roof uplift connections designed for the basic wind speed of the location. The trusses were also

nailed to head plates of the internal walls that crossed them. The bottom chord of the gable-end truss was nailed to the head plate at 0.4m (16 inches) on center in addition to the roof uplift connectors provided at each of its ends. The nailing connections, openings in the wall, stud and sheathing configurations were provided such that a continuous load path would be provided from the roof to the foundation.

3. FINITE ELEMENT MODEL

3.1 Modeling of structural components

Extensive work has been performed on finite element modeling of a light-framed conventional timber construction in the past. Importance has been given to the modeling of shear walls, materials and interconnection components as they consist of the main and critical load bearing components. Kasal et al. (1994) stated in his work that the shear wall load sharing is a function of shear wall stiffness, roof diaphragm action and inter-component stiffness. Collins (2005) used shell elements with only plate stiffness for wall sheathing and beam elements with axial and bending stiffnesses for beams and studs. Nonlinear springs were used to represent nonlinearities in connections. Roof and floor diaphragms were represented by shell elements with shear and membrane stiffness. Paevere et al. (2003) modeled the roof as a rigid diaphragm that contributed significantly to the lateral load sharing and also proved that transverse walls did not contribute to load sharing among shear walls. He et al. (2001) modeled the panel as a 3D thin plate element and the frame as a 3D beam with inelastic material properties.

For the present study, the ANSYS finite element software was used for the FE analysis. The shell element which has shear, bending and membrane stiffnesses was chosen to represent the sheathing. This element is an 8-node quadrilateral structural shell with 6 degrees of freedom per node (ANSYS). The beam element used to model the studs has axial and bending stiffnesses and also has 6 degrees of freedom per node (ANSYS). Elastic material properties were used for both the shell and the beam elements. Nonlinear springs were used to model the connections. Each connection was replaced by three independent nonlinear springs with zero length to account for one axial and two lateral stiffnesses (ANSYS). The nonlinear spring stiffness values were obtained by running strength tests on

different connection configurations as discussed in next section. The main frame of the building was modeled in great detail. The trusses were modeled as one complete unit to resemble construction practices on site. The nodes on the sole plate were given fixed boundary conditions simulating anchorage to the ground. The roof and wall diaphragms were modeled panel by panel, to simulate the same effects as in the field without over-estimating diaphragm stiffness.

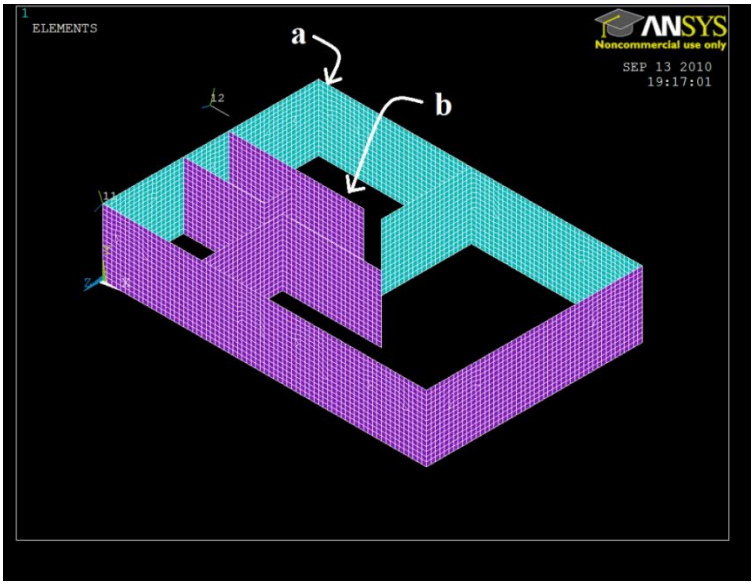

Fig. 3. Base of FE model with points ‘a’ and ’b’

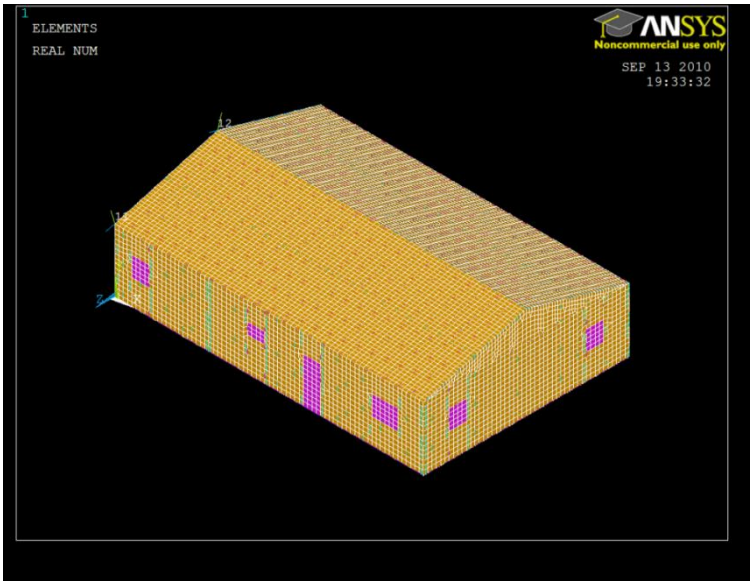

Fig. 4. Complete FE model of example building

Fig. 3 shows the FE model of the base of the example building and the points ‘a’ and ‘b’ referenced later in the paper, in section 4.2. Point ‘a’ is on the external surface of the wall of the building and ‘b’ is on the floor inside the building. Fig. 4 shows the complete FE model of the building.

3.2 Modeling of nonlinear spring connection

As mentioned before, experiments were performed to get the stiffness curves of different nail connections. Aune (1986) stated that nails only under lateral loads alone fail due to either yielding by nail bending or wood crushing or both. All these failure modes were observed in the laboratory tests performed. The testing was performed in accordance with the guidelines of “Standard Test Methods for Mechanical Fasteners in Wood” ASTM-D1761- 06 (2008). For tests measuring lateral stiffnesses, a hole of slightly smaller diameter than that of the nail’s, was pre-drilled in the wood and the nail head was positioned slightly above the surface. This almost eliminated the axial effects caused by friction between the nail and the wood and nail head fixity, thereby, causing the lateral stiffness to be quite independent of the axial stiffness.

The nail connections tested in the structures laboratory of the department of aerospace engineering at ISU can be classified into four types: head/sole plate to studs, blocking to head plate, sheathing to beam/stud and special type uplift connector to head plate. Each of these connection types was tested for one axial and two lateral nonlinear stiffnesses and ten samples were tested per set. Once the stiffness values were obtained, the non-oriented spring pair model (Judd, 2005) was used to represent the nail connection in the FE model. Fig. 5 shows the stiffness curves for the head/sole plate to stud configuration and Fig. 6 shows the experimental setup to measure the axial stiffness for the same. Figs. (1-3) in the appendix to this chapter show the stiffness curves of all the other nail configurations.

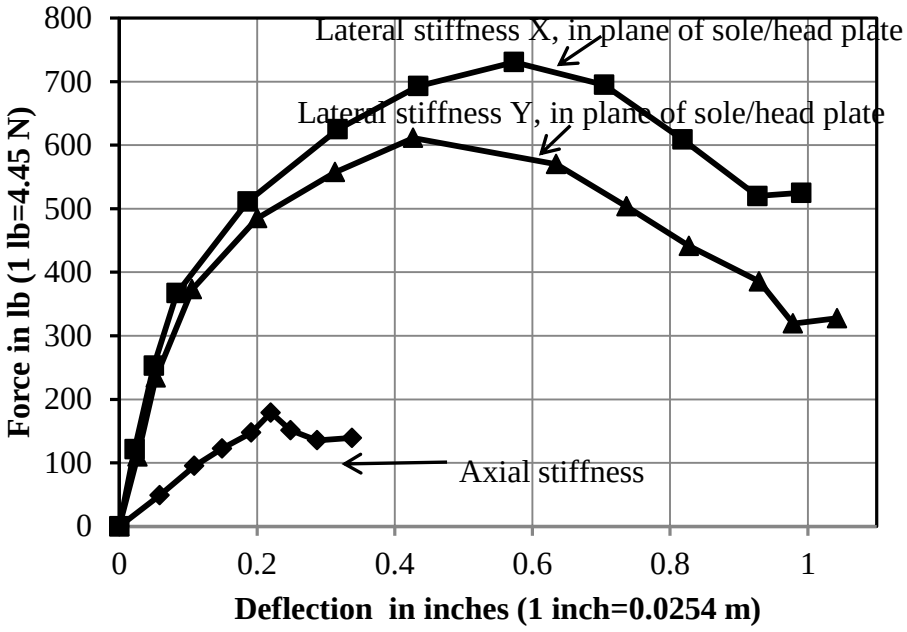

Fig. 5. Stiffness curves for head/sole plate to stud configuration (2-16d common end-nails)

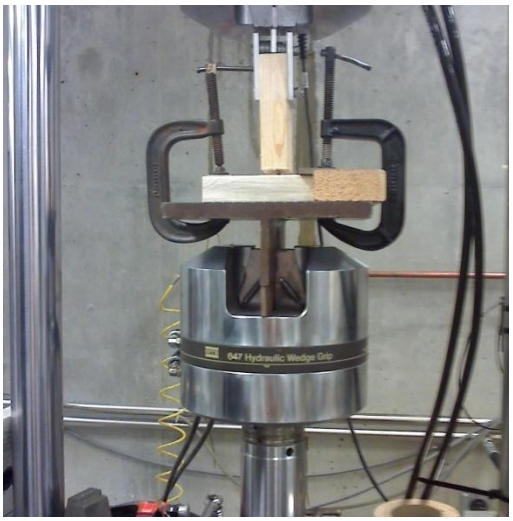

Fig. 6. Experimental setup for head/sole plate to stud configuration

4. EXPERIMENTAL EVALUATION OF TORNADIC WIND EFFECTS

4.1 Tornado simulator settings

The ISU's Tornado/Microburst Simulator was used for the experimental study. The detailed description of the simulator can be found in Haan et al. (2008). The 'Vane 5'settings were used for this experiment (Haan et al., 2008). The translating tornado-like vortex that was

simulated had a swirl ratio of 1.14, core radius of 0.53 m (r_c), where the maximum tangential velocity ($V_{\Theta max}$) occurs, and $V_{\Theta max}$ of 9.7 m/s. The translation velocity of the tornado was fixed at 0.30 m/s to obtain the most critical transient effects (Sengupta et al., 2008) on the external and internal pressures for the building model. The building started experiencing noticeable loads when the center of the tornado reached a distance of $4r_c$ with respect to (w.r.t.) the building center. Hence, this position of the tornado was taken as the starting point for the analysis in this paper. For the FE analysis, the loads corresponding to a translating tornado i.e., the dynamic pressure readings were used.

4.2 Pressure model details

A building model, representing the residential building, partially damaged in the Parkersburg tornado as mentioned before, was built with a geometric scale (λ_L) of 1:75 and was used with the 'Vane 5' tornado settings (higher swirl ratio) as described in Haan et al. (2008) to preserve the similarity with the Parkersburg EF5 tornado. The tornado vortex velocity scale (λ_V) was estimated to be 1:8 corresponding to a velocity of 89.4 m/s (200 mph), 3-sec gust. Also, using λ_L, the tornado core-radius scales up to about 40 m which is less than the predicted core-radius of the Parkersburg EF5 tornado that was estimated to be about 130 m. For all the tests, the building model was located at an offset distance of $1.42r_c$ from the centerline of the tornado path on its left side, because the example building chosen for this study that got partially damaged in the Parkersburg tornado was around that location w.r.t. its centerline (~200 m). As a tornado of smaller radius was found to cause higher peak loads than a tornado of larger radius (Sengupta et al., 2008), the FE model that uses the experimental pressure data is expected to see similar or more severe damage than the building damaged by the Parkersburg tornado. The translation velocity 0.30 m/s in the lab scales up to 23 m/s using the chosen length scale λ_L and the time scale (λ_t) of 1 as justified in Haan et al. (2008), which compares well with the translation velocity of the Parkersburg tornado (~16.5 m/s). The internal volume was scaled to maintain the similarity of the dynamic response of the volume at model scale to that in full scale (Holmes, 1978). The internal volume scale (λ_{vol}) was calculated as follows:

$$\lambda_{vol} = \frac{{\lambda_L}^3}{{\lambda_V}^2} \quad (1)$$

In order to achieve this similarity, a sealed volume chamber was installed at the bottom of the model so that the internal volume was increased proportionally based on the scaling law above. The model contained 127 pressure taps, 122 on the exterior of the building to measure external pressures and 5 inside the building at different locations to capture internal pressure in different building chambers.

Dominant openings like doors (2) and windows (11) were provided in the model and could be sealed when needed to simulate the effect of closed windows and doors. As described later in this paper (Sections 5.1.3, 5.1.4), experimental pressure readings were required for the prototype building with 40% and 100% of its roof pulled out and with different doors/windows opened and closed. The building model 1 of Fig. 7 shows the model with the entire roof and with partial openings (1 door and 1 window). The building model 2 of Fig. 7 shows the model with 40% of its roof pulled out and with 1 open door and 4 open windows. Building model 3 of Fig. 7 shows the model with the entire roof pulled off, with 1 open door and 4 open windows.

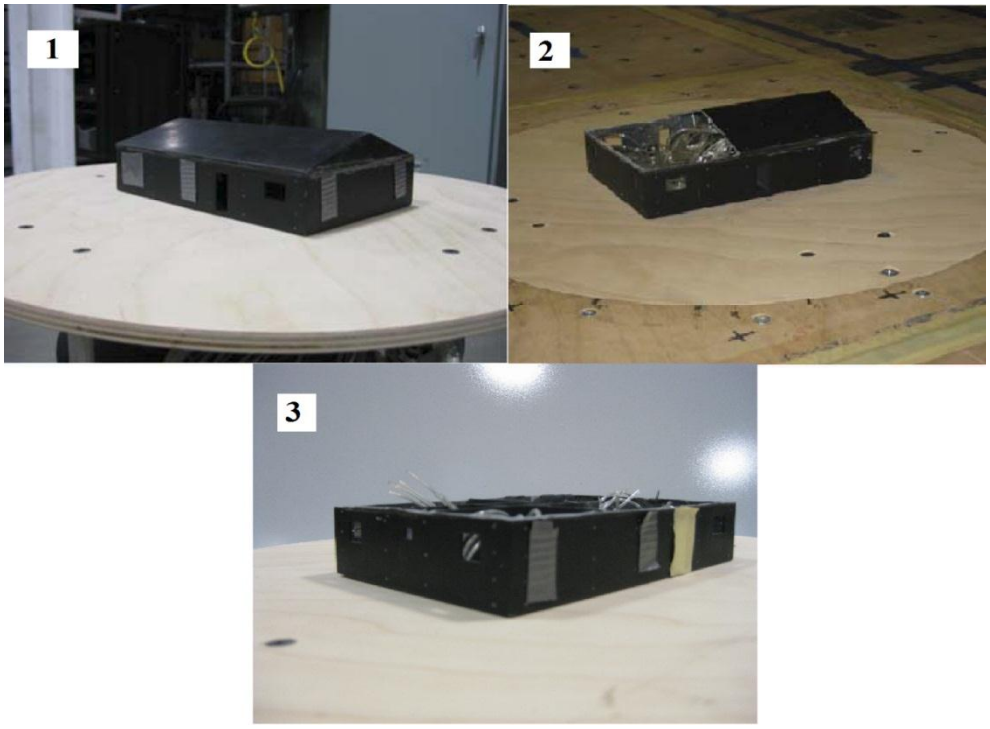

Fig. 7. Experimental models with partial openings

Two high-speed 64-channel electronic pressure scanners (Scanivalve ZOC33/64Px) were used to measure the pressure distribution on the building model. A total of 3125 data points were collected over 20 seconds (sampling rate~156 Hz) for the translating tornado. The averaged pressure readings over three identical runs per case were obtained. The initiation of data acquisition and the crane movement for the moving case was synchronized using a common external trigger.

4.2 Effect of internal pressure, leakage and position

The internal pressure plays a major role in the net pressure acting on various structural components in a tornado. This completely changes the failure modes of the structure subjected to the tornado-induced wind loads. The experimental model was situated to the left of the translating tornado with wind swirling in the anti-clockwise direction. The building's major axis (X) is in the direction of the translating tornado and its minor axis (Y) is orthogonal to X in the swirling direction of the tornado. The axis Z is taken pointing up as shown in Fig. 8. These were taken as the global axes and the origin is situated at the center of the building. All distances are w.r.t. these axes in this paper.

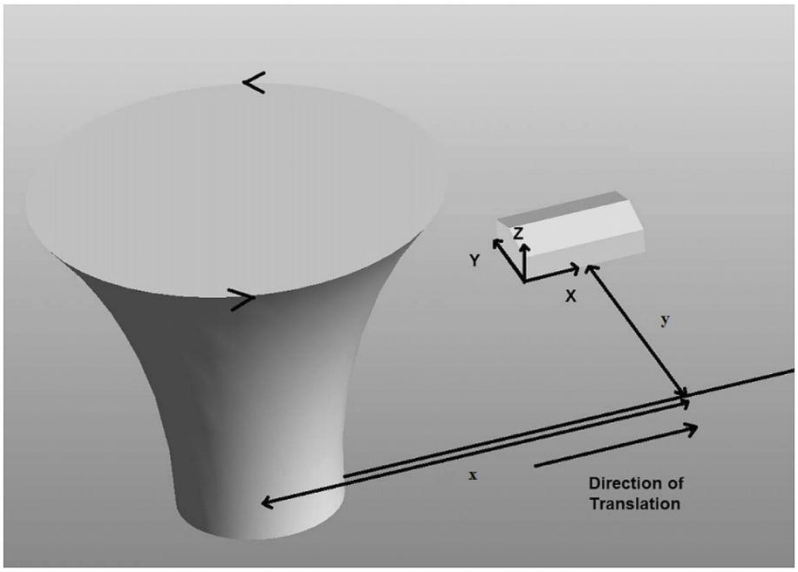

Fig. 8. Position of experimental model w.r.t the translating tornado

The location of the center of the tornado w.r.t. the center of the building is specified in terms of distances *x* and *y*, measured along X and Y, respectively. Fig. 8 shows the position of experimental model w.r.t the translating tornado and is similar in position and orientation to the partially damaged example building at Parkersburg.

To study the effect of internal pressure in a tornado, tests were conducted with different model opening configurations. The three most significant test cases for this analysis are discussed here: (1) sealed building (closed doors and windows; not fully sealed because of porosity in the cladding) (2) open building (with all doors and windows open) (3) dominant opening (with only one open door). The time series of the pressure coefficients, as the tornado translates at a speed of 0.30 m/s, were obtained. It was found more useful for this work to observe the pressure as a function of the distance *x*, normalized w.r.t. core radius r_c instead of observing it as a function of time. The curves in Fig. 9 (a-c) give the external and internal pressure coefficients: Cp_e at 'a' and Cp_i at 'b' (Fig. 3), respectively, and the net pressure coefficient $Cp_{net}= Cp_e-Cp_i$ for the three test cases mentioned above. The pressure coefficients are defined by Eqn. 2.

$$Cp = \frac{\Delta p}{0.5\rho V_{\theta max}{}^2} \tag{2}$$

where, Cp = pressure coefficient, Δp = differential pressure (Pa) = p-p_s, where p is external p_e or internal pi pressure and p_s is atmospheric static pressure inside the lab away from the tornado; $V_{\theta max}$=maximum tangential velocity (9.7m/s).

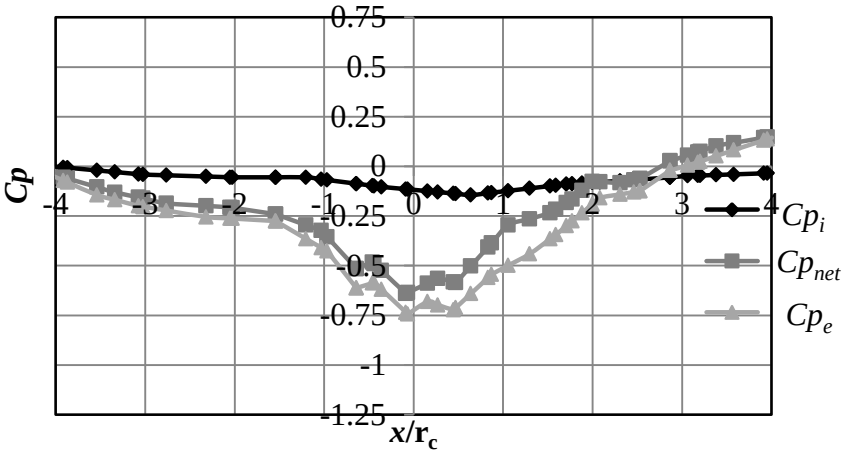

Fig. 9(a). Effect of internal pressure – test case 1

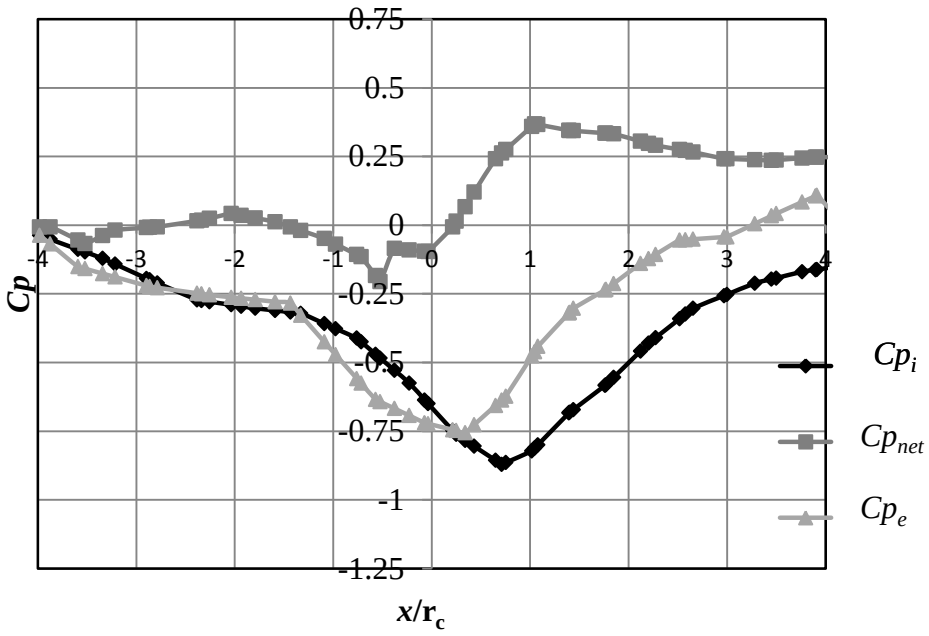

Fig. 9(b). Effect of internal pressure – test case 2

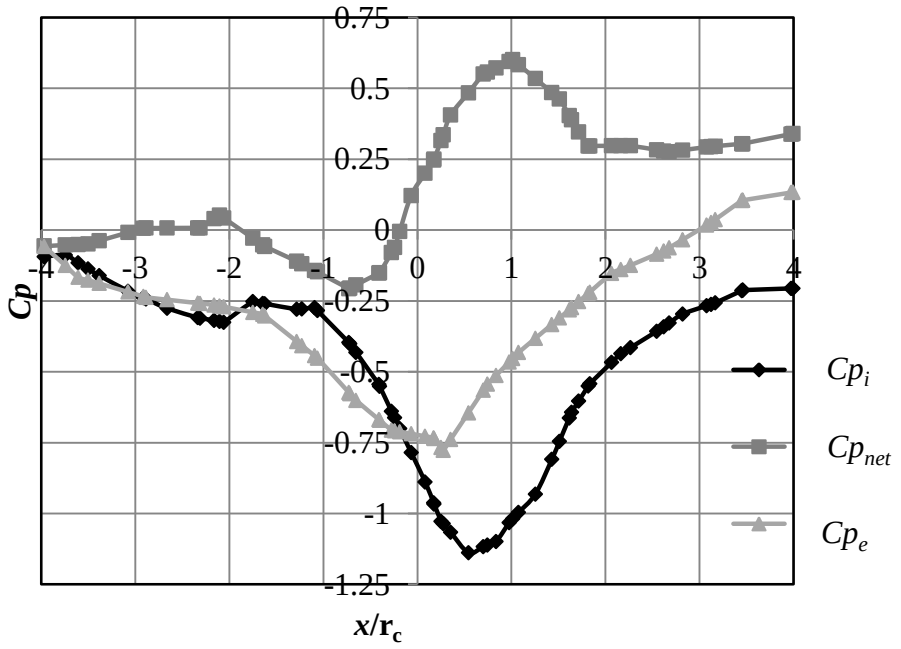

Fig. 9(c). Effect of internal pressure – test case 3

The results in Fig. 9 (a-c) show that the net pressure coefficient Cp_{net}, acting outside on the wall at'a', in a tornado, changes considerably when the internal pressure is taken into

account. The sealed building has a minimum amount of porosity in it and hence a low negative internal pressure, Cp_i, at 'b' (suction inside the building), leading to a high net negative pressure (Cp_{net}) acting outside on the wall (at 'a'). In the second test case (open building), a positive net pressure (Cp_{net}) is seen to develop outside on the wall (at 'a') of the building and in the case of the dominant opening, the net pressure (Cp_{net}) outside on the wall (at 'a') reaches a positive maximum. As the pressure pattern takes a drastic change due to the effect of internal pressure in different cases, the failure modes and final damage state of the building seen in these cases are expected to vary. Hence, this effect which would greatly influence the wind's interaction with the structure has to be captured.

Fig. 10 shows the internal pressure coefficient, Cp_i, at point 'b' (Fig. 3) as a function of *leakage* and *position* when the tornado is at a location, x=0. *Leakage* is defined here as the percentage ratio of the total opening area to the total surface area of the building. The porosity that is present due to material properties is ignored in the calculation. The *position* defines the location of the opening on the building. It can be noted that the internal pressure varies with position and therefore it is necessary to know the position of the opening formed due to the loss of cladding material or other failures to capture the updated wind's interaction with the structure and thereby accurately predict the modes of failure. In this work, the position is determined by the FE analysis as described later (Section 5.1.1). The negative maximum internal pressure coefficient, Cp_i, seen in Fig. 10 corresponds to the dominant opening case (only one open door). From the study performed, it was concluded that the modes of failure vary with different building opening configurations and hence two major cases were chosen to predict the final damage state, to be compared with that of the example building partially damaged at Parkersburg: (1) sealed building and (2) building with a partially fixed (loosely shut) door. The second case was chosen to simulate a possible dominant opening situation during the passage of the tornado.

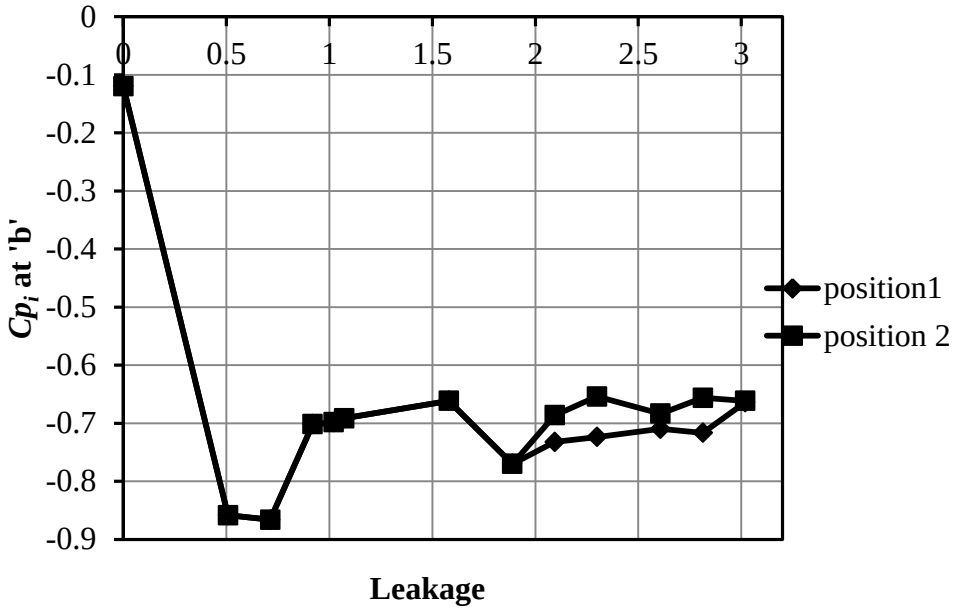

Fig. 10. Internal pressure as a function of leakage and position

5. ANAYSIS OF FAILURE MODES

5.1 Finite element analysis

5.1.1 Methodology

The wind loads used in the analysis correspond to that of an EF5 tornado with wind speeds of 89.4 m/s (200 mph), 3-sec gust, calculated with the pressure coefficients measured in the laboratory to preserve similarity with the Parkersburg tornado as described before. For the first FE analysis, the dynamic wind pressures on the sealed building model located at x= -4r_c and y= -1.42r_c w.r.t the translating tornado were taken as input. It was assumed that the surface area immediately around a pressure tap saw the same pressure value. The net pressures (external minus internal) were applied to the corresponding areas of the FE model of the prototype building and the first FE analysis was performed. If any failure of building components was observed in the FE analysis, the corresponding component in the building prototype was removed. A fresh set of experiments were performed with the model of the modified prototype and updated pressure readings were taken. Thus, the wind's interaction with the partially damaged structure as seen on the site was preserved. For the second FE analysis, the updated pressure readings corresponding to the tornado's position, x= -3.5r_c and

y= -1.42r_c were used. This corresponds to a time increment of approximately one second. The process was thus repeated until the tornado reached a position, x=+4r_c and y= -1.42r_c and the final damaged state was noted to be compared with that of the example building at Parkersburg. While the tornado was close to the building (x= -2r_c to x=+2r_c), pressure readings were applied, corresponding to time increments of quarter to half a second, depending on the intensity of the loading. The maximum damage (for both the cases: sealed building, building with partially fixed door) occurred in this range and therefore had to be closely monitored. For higher load/time steps where the nodes of the elements experienced large displacements, the FE analysis encountered solution instabilities. To improve the solution stability, the Line Search preference (ANSYS) was used along with the Newton-Raphson procedure.

5.1.2 Failure criteria

The failure criteria of the structural components were chosen as follows – in accordance with guidelines of "Standard Test Methods for Mechanical Fasteners in Wood" ASTM-D1761-06 (2008), the nails that exceeded a relative displacement (pullout) of 2 cm were considered to have experienced complete failure. The buckling load was used for the studs and flexural and shear strength was used for sheathing as references of failure. In addition to checking for loads, excessive deflection was also used as reference of failure for studs and sheathing components. The failure criterion of the connections was slightly modified so as not to overestimate their strengths. Failure of any one of the nonlinear springs was considered as failure of the entire connection. The stiffness of these failed components were explicitly set to zero in the next FE analysis, i.e., they were physically removed from the structure for the next analysis corresponding to the incremented time and location of the tornado. When the damage of the panel was less than 40% based on either stresses, deflection or connection failure criterion, only the stiffness values of these failed components were set to zero in the next FE analysis. When the damage of the panel exceeded 40%, not only were the stiffness values of these corresponding failed components set to zero in the next analysis, but the updated pressure readings obtained with these components removed from the prototype (mentioned in section 5.1.1) were also used for the next analysis. The initial failure modes

were identified as axial connection (e.g. nail) pullout, shear failure of sheathing, gable end failure and failure at wall junction or corner stress concentration points. The final failure modes included axial or lateral connection failure, shear or flexural failure of sheathing material and bending failure in beams and studs.

5.1.3 Sealed building

Analyses were performed for the sealed building under two conditions: building with only minimum roof uplift connectors specified by IBC (2006) and building with roof uplift connectors designed for 40m/s (90 mph), 3-sec gust wind as mentioned in section 2. A program was written to calculate the approximate lateral wind velocity seen at the building's location as the tornado translates by. For the building case with minimum roof uplift connectors, more than 40% of the uplift connectors failed and hence the roof experienced partial pullout failure at its connections to the wall as expected, even at~38 m/s (85 mph), 3-sec gust, corresponding to the tornado's location, $x = -2.5r_c$. For the building with roof uplift connectors designed for 40m/s (3-sec gust), the uplift connectors failed in a similar way and the roof experienced partial pullout failure, but it happened at~45 m/s (100 mph), 3-sec gust, corresponding to the tornado's location, $x = -2r_c$. The roof experienced complete pullout at~56 m/s (125 mph), 3-sec gust, corresponding to $x = -1.65r_c$. The wall sheathing in both the cases experienced a low degree of damage. Once the roof experienced complete pullout, the net pressure dropped and the building did not experience any further noticeable damage except for a slight failure in the wall sheathing. Fig. 11(a) shows the Von Mises stresses (in ksi, 1 ksi=6.895 MPa) developed in the final damage state of the sealed building case (roof uplift connectors designed for 40 m/s (3-sec gust)) with the failed roof elements removed. As can be seen, the gable end at the right side of the building (positive *x*-plane, Fig. 8) has been pulled off completely along with most of the roof. Only parts of the left gable end remain standing. Fig. 11(b) shows the partially damaged example building at Parkersburg and they compare well. Figs. (4-7) in the appendix to this chapter show the detailed nodal displacements (X, Y and Z) and Von Mises element stresses in the sealed building, with roof uplift connectors designed for 40 m/s (3-sec gust), for different tornado locations w.r.t. the building.

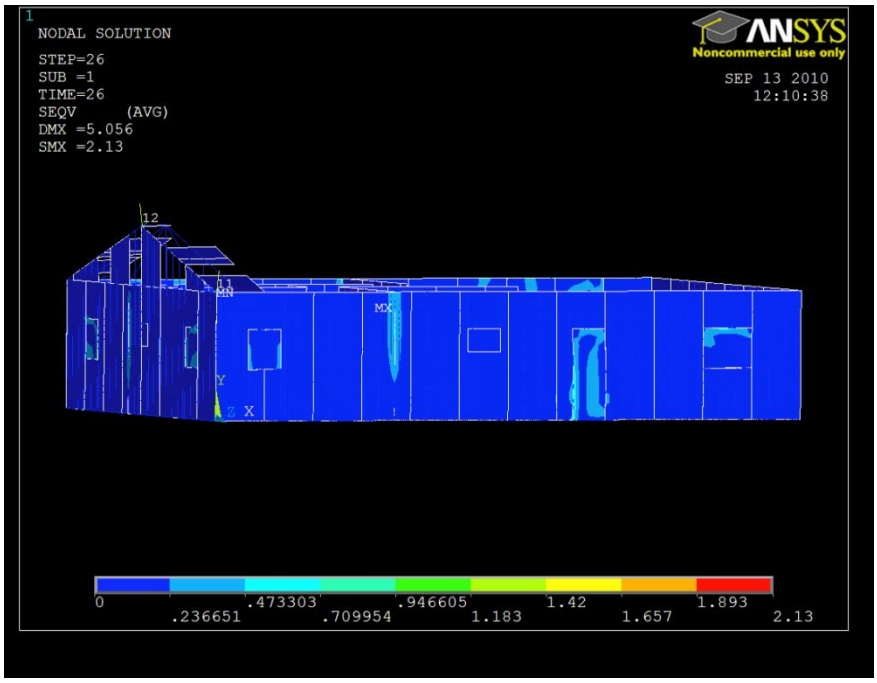

Fig. 11(a). Final damage state of sealed building with roof uplift connectors designed for 40 m/s (3-sec gust), with failed roof elements removed

Fig. 11(b). Partially damaged example building at Parkersburg

5.1.4 Building with partially fixed door

Similar analyses were performed for the building with a partially fixed door (shown in Fig. 12) simulating the effect of loosely shut door with roof uplift connectors designed for 40 m/s (3-sec gust). At x= -3.5r_c, the partially fixed door opened up and from then on the pressure pattern experienced a drastic change due to the effects of increased negative internal pressure as seen in section 4.2. The failure modes observed here varied greatly when compared to that noted in the sealed building. For a wind speed of~80 m/s (180 mph), 3-sec gust, corresponding to the tornado's location, x=+0.25r_c, the gable end at the right side of the building and the wall below it caved in. Some of the beams and studs in the wall and in the trusses near the right gable end experienced failure due to bending. Uplift connectors near the right gable end experienced pullout and lateral failure. The sheathing on the left and right walls, perpendicular to the direction of translation of the tornado experienced intermediate damage due to nail pullout or shear and flexural failure, while the sheathing on the other walls and the roof experienced a low degree of damage. At this point, as the right gable end and the wall below it experienced complete failure, the net pressure dropped. From this point forward, no noticeable damage was observed as the tornado moved away from the building. Fig. 12 shows the Von Mises stresses (in ksi, 1ksi = 6.895 MPa) developed in the building with a partially fixed door at x=+0.25r_c. The gable at the right end and the wall below it can be seen caving in. This was the maximum damage witnessed by the building. For better representation of failure of the building in Fig. 12, but for the door, the failed elements have not been removed. The final damage state of this case did not compare well with the partially damaged example building at Parkersburg.

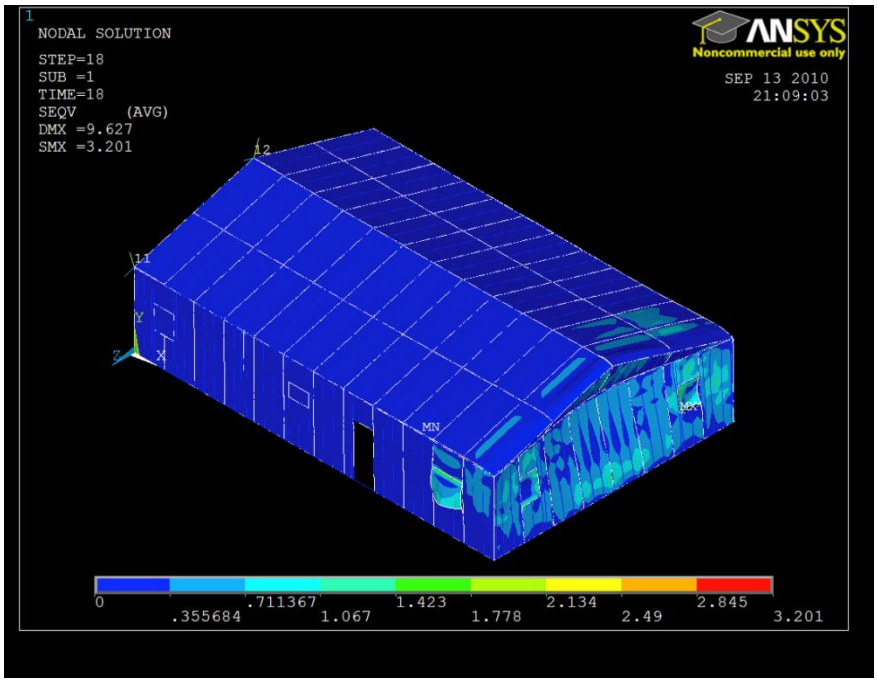

Fig. 12. Damage state of building with partially fixed door at $x = +0.25r_c$, with failed elements removed

From the analyses it can be noted that different failure modes occur for the building with the same design and for the same tornado, based on different failure paths the building takes. Hence, this provides better understanding in assessing the intensity of the tornado from the observed damage state of the building. Figs. (8-11) in the appendix to this chapter show the detailed nodal displacements (X, Y and Z) and Von Mises element stresses in the building, with a partially fixed door, for different tornado locations w.r.t. the building.

5.1.5 Analyses with EF4 and EF3 tornados

It was necessary to determine if a tornado of lower intensity could cause the same amount of damage for assessing the right intensity of the tornado from the observed damage state of the building. Therefore, the same analysis as performed with a sealed building with uplift connectors designed for 40 m/s, 3-sec gust for an EF5 tornado was repeated for EF4 and EF3 tornados. The same experimental pressure coefficients as used for the EF5 case were used to estimate the loads for EF3 and EF4 tornados corresponding to 60 m/s (136 mph) and 74 m/s (166 mph), respectively. The same tornado radius and building position were maintained. Although the internal volume scale (λ_{vol}) should be adjusted because of a change in velocity

scale (Eqn. 1) and experiments repeated, it could be justified not to do so because leakage (small openings) did not play an important role until the failure in these cases (Oh et al., 2007).

From the analyses it was noted that the tornado of intensity EF4 caused similar damage to the sealed building as EF5, but with a slightly smaller degree of damage. The roof experienced complete pullout but the wall sheathing had a lower degree of damage. The tornado of intensity EF3 followed the failure mode as expected but the uplift connectors that failed were not sufficient to cause complete roof pullout and the wall sheathing had the least damage. Most of the components sustained very little deformation after the tornado crossed the building. In this study, it can be concluded that a tornado of intensity EF4 could have been sufficient to inflict the same degree of damage as seen in the partially damaged example building at Parkersburg. This knowledge improves the ability to assess the intensity of a tornado from the observed damage state.

6. CONCLUSION

A partially damaged one-story building, located within the damage path of the Parkersburg EF5 tornado (May 25, 2008), was chosen for analysis using FE and comparison of observed damage to those predicted in this study. The dynamic internal and external pressures on the building as the tornado translates by the building were assessed with a geometrically scaled model (1:75) of the building placed in the ISU's Tornado/Microburst Simulator. A detailed finite element analysis of the building was performed with pressure data at a given tornado location. The following conclusions can be drawn.

1. This work predicted the stage-wise failure of the structural components of a gable-roofed timber building when hit by a tornado.
2. The methodology described here enables accurate damage prediction and failure of a low-rise building from a tornado that will improve its component design and construction.
3. The study provided a better understanding of the influence of dynamically varying internal pressure on the building performance during a tornado.

4. It helped in assessing the intensity of a tornado from the observed damage state of the building.
5. Uplift connectors designed for resisting 90 mph straight line wind as per building code barely resist 90 mph tornado wind in a sealed building. Understanding modes of failure can improve future construction practices.
6. Leakage and openings influence net wind loads and hence are vital for alleviating tornado induced damage.

It is encouraging that the effects of debris in a tornado be implemented in a similar study in an analysis on a group of buildings in different terrains to see the changes in modes of failure and to improve the understanding of the EF scale. The performance of new and lightweight materials as different structural components and improved connections to reduce the damage intensity in a tornado can be studied. As there has been an improved knowledge in the influence of openings on net wind loads in a tornado, studies can be performed to optimize the internal and external geometry of the building to reduce net wind loads in a tornado. The effect of turbulence in the wind loads of a tornado and the sudden formation of openings need to be incorporated to capture more accurately the effects of the dynamic wind's interaction with the structure.

ACKNOWLEDGEMENTS

This research was funded by National Oceanic and Atmospheric Administration (NOAA) Award # NA08OAR4600887. We gratefully acknowledge the work of Bill Rickard and numerous undergraduate students from the ISU Aerospace Engineering Department who contributed to this project.

REFERENCES

AF&PA, 2001. Details for conventional wood frame construction, 2001. American Forest and Paper Association.

ANSYS. Academic research 12.1, help system, ANSYS Inc.

APA, 1997. Plywood Design Specifications 1997. APA, The Engineering Wood Association.

ASTM-D1761-06, 2008. Annual book of ASTM standards 2008-standard test methods for mechanical fasteners in wood, ASTM International.

Aune, P., Mallory, M.P., 1986. Lateral load-bearing capacity of nailed joints based on the yield theory-experimental verification. United States Department of Agriculture, Research Paper FPL 470.

Chang, C.C., 1971. Tornado wind effects on buildings and structures with laboratory simulation. Proceedings of the Third International Conference on Wind Effects on Buildings and Structures, Tokyo, 213–240.

Collins, M., Kasal, B., Paevere, P.J., Foliente, G.C., 2005. Three-dimensional model of light frame wood buildings I: model description. Journal of Structural Engineering 131, 676-683.

Dutta, P.K., Ghosh, A.K., Agarwal, B.L., 2002. Dynamic response of structures subjected to tornado loads by FEM. Journal of Wind Engineering and Industrial Aerodynamics 10, 55-69.

Haan, F.L., Sarkar, P.P., Gallus, W.A., 2008. Design, construction and performance of a large tornado simulator for wind engineering applications. Engineering Structures 30, 1146-1159.

He, M., Lam, M., Foschi, R.O., 2001. Modeling three-dimensional timber light-frame buildings, Journal of Structural Engineering, 127, 901-913.

Holmes, J.D., 1978. Mean and fluctuating internal pressures induced by wind, Wind Engineering Report 5/78. Department of Civil and Systems Engineering, James Cook University of North Queensland, Australia.

IBC, 2006. 2006 International Building Code. International Code Council, Inc.

Jischke, Light, 1983. Laboratory simulations of tornadic wind loads on a rectangular model structures. Journal of Wind Engineering and Industrial Aerodynamics 13, 371–382.

Judd, J.P., Fonseca, F.S., 2005. Analytical model for sheathing-to-framing connections in wood shear walls and diaphragms. Journal of Structural Engineering 131, 345-352.

Kasal, B., Leichti, R. J., Itani, R.Y., 1994. Nonlinear finite-element model of complete light-frame wood structures. Journal of Structural Engineering 120, 110-119.

Kumar, N., 2008. Stress analysis of wood-framed low-rise buildings under wind loads due to tornados. Master of Science thesis, Iowa State University.

Mehta, K.C., Mcdonald, J.R., Minor, J., 1976. Tornadic loads on structures. Proceedings of the Second USA–Japan Research Seminar on Wind Effects on Structures, Tokyo, Japan, 15–25.

Oh, J.H., Kopp, G.A., Inculet, D.R., 2007. The UWO contribution to the NIST aerodynamic database for wind loads on low buildings: Part 3. Internal pressures. Journal of Wind Engineering and Industrial Aerodynamics 95, 755-779.

Paevere, P.J., Kasal, B., Foliente, G.C., 2003. Load-sharing and re-distribution in a one-story wood frame building. Journal of Structural Engineering 129, 1275–1284.

Sarkar, P.P., Kikitsu, H., 2008. Damage survey report on Parkersburg and New Hartford, Iowa, EF5-tornado of May 25, 2008.

Savory, E., Parke, G.A.R., Zeinoddini, M., Toy, N., Disney, P., 2001. Modeling of tornado and microburst-induced wind loading and failure of a lattice transmission tower. Engineering Structures 23, 365-375.

Sengupta, A., Haan, F.L., Sarkar, P.P., Balaramudu, V., 2008. Transient loads on buildings in microburst and tornado winds. Journal of Wind Engineering and Industrial Aerodynamics 96, 2173-2178.

Sparks, P.R., Hessig, M.L., Murden, J.A., Sill, B.L., 1988. On the failure of single storied wood framed houses in severe storms. Journal of Wind Engineering and Industrial Aerodynamics 29, 245–252.

Ward, N.B., 1972. The exploration of certain features of tornado dynamics using a laboratory model. Journal of the Atmospheric Sciences 29, 1194–204.

Wen, Y.K., 1975. Dynamic Tornadic wind loads on tall buildings. American Society of Civil Engineers, Journal of the Structural Division 101, 169–185.

Wen, Y.K., Ang, A.H.S., 1975. Tornado risk and wind effects on structures. Proceedings of the Fourth International Conference on Wind Effects on Buildings, Heathrow, pp. 63– 74.

WFCM, 2006. Guide to wood construction in high wind areas for one- and two- family dwellings. American Forest and Paper Association.

Matweb, 2010. http://www.matweb.com, September 14, 2010.

APPENDIX

FIGURES REFERNCED IN CHAPTER 3

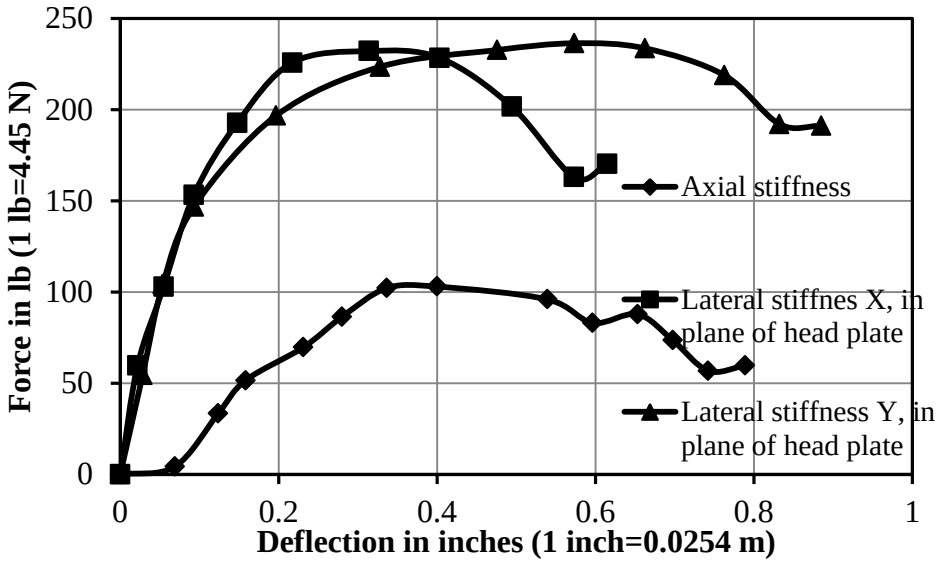

Fig. 1. Stiffness curves for blocking to head plate configuration (1-8d common toe-nail)

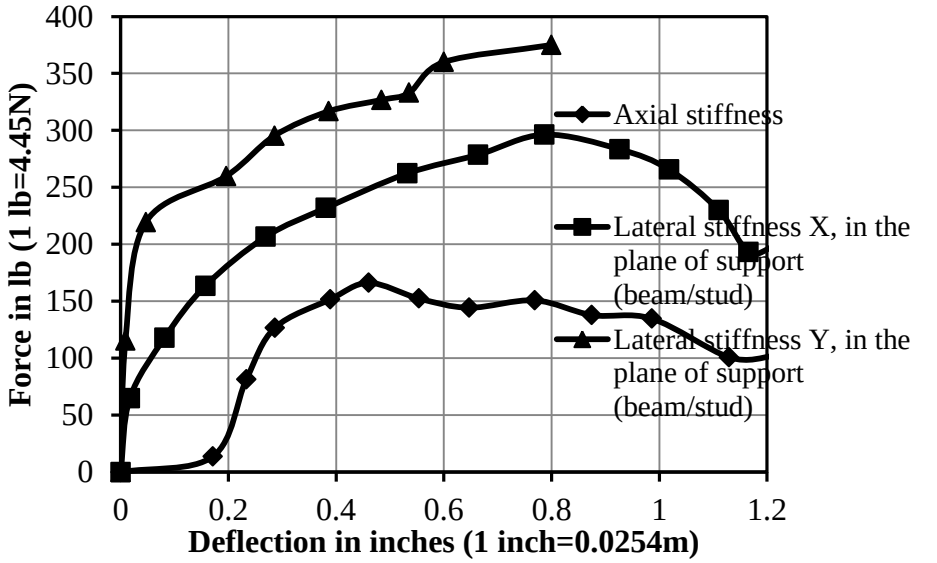

Fig. 2. Stiffness curves for sheathing to support (beam/stud) configuration (1-8d common face-nail)

Note: Principal axis of sheathing perpendicular to major axis of support of length 'l'. Sheathing undergoes one-way deflection, as l>b, where, b=length of shorter support.

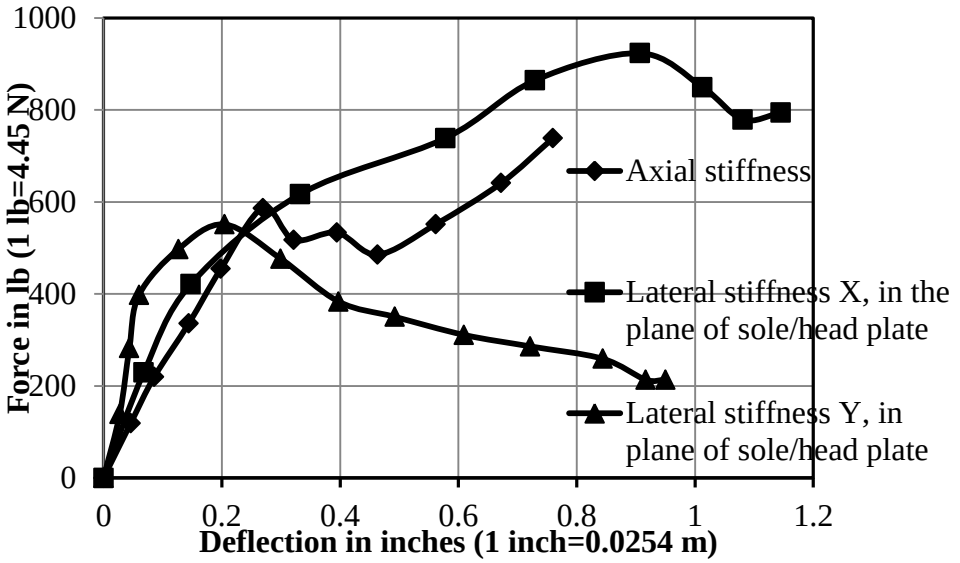

Fig. 3. Stiffness curves for special type uplift connector to head/sole plate (3-8d common toe-nail and 1-Simpson A35[2] connector)

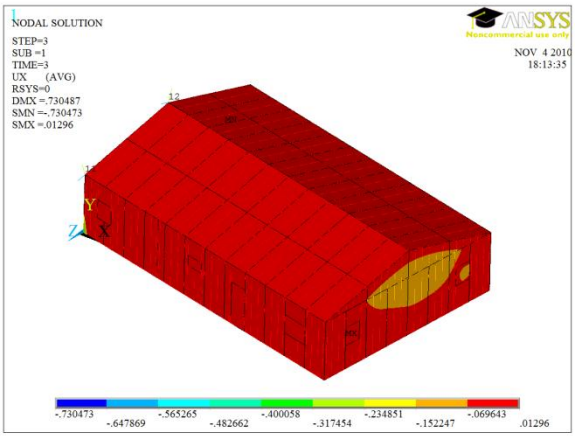

x= -4r_c

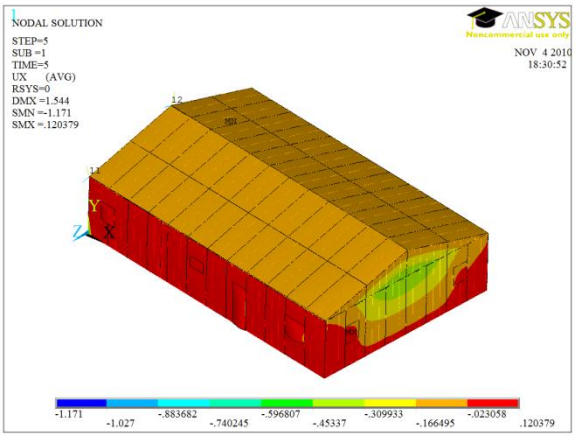

x= -3r_c

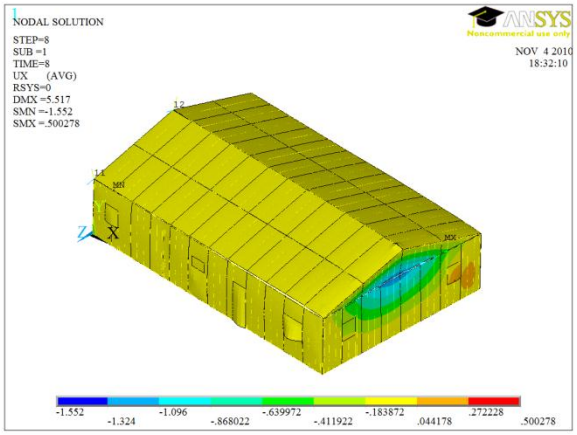

x= -2r_c

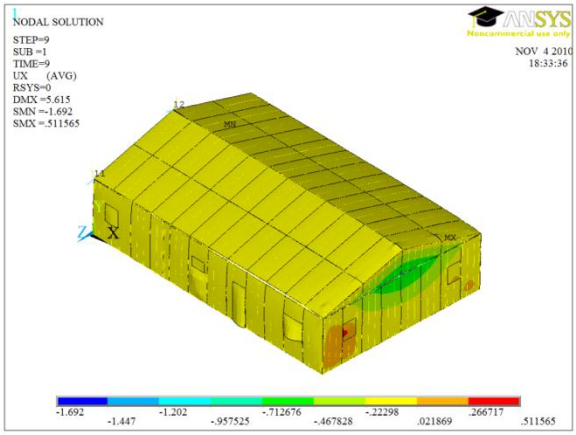

x= -1.65r_c

Fig. 4. Nodal displacement in the X direction for building faces on the +X, –Y and +Z planes for different tornado positions w.r.t. the center of the building (sealed building)

Note: Blue represents negative displacement and red represents positive displacement on the X axis. The failed elements have not been removed in these plots. For better representation of failure in the figures, the scale of the deformation used for plotting has been magnified. Deflection is in inches (1 in=0.0254 m).

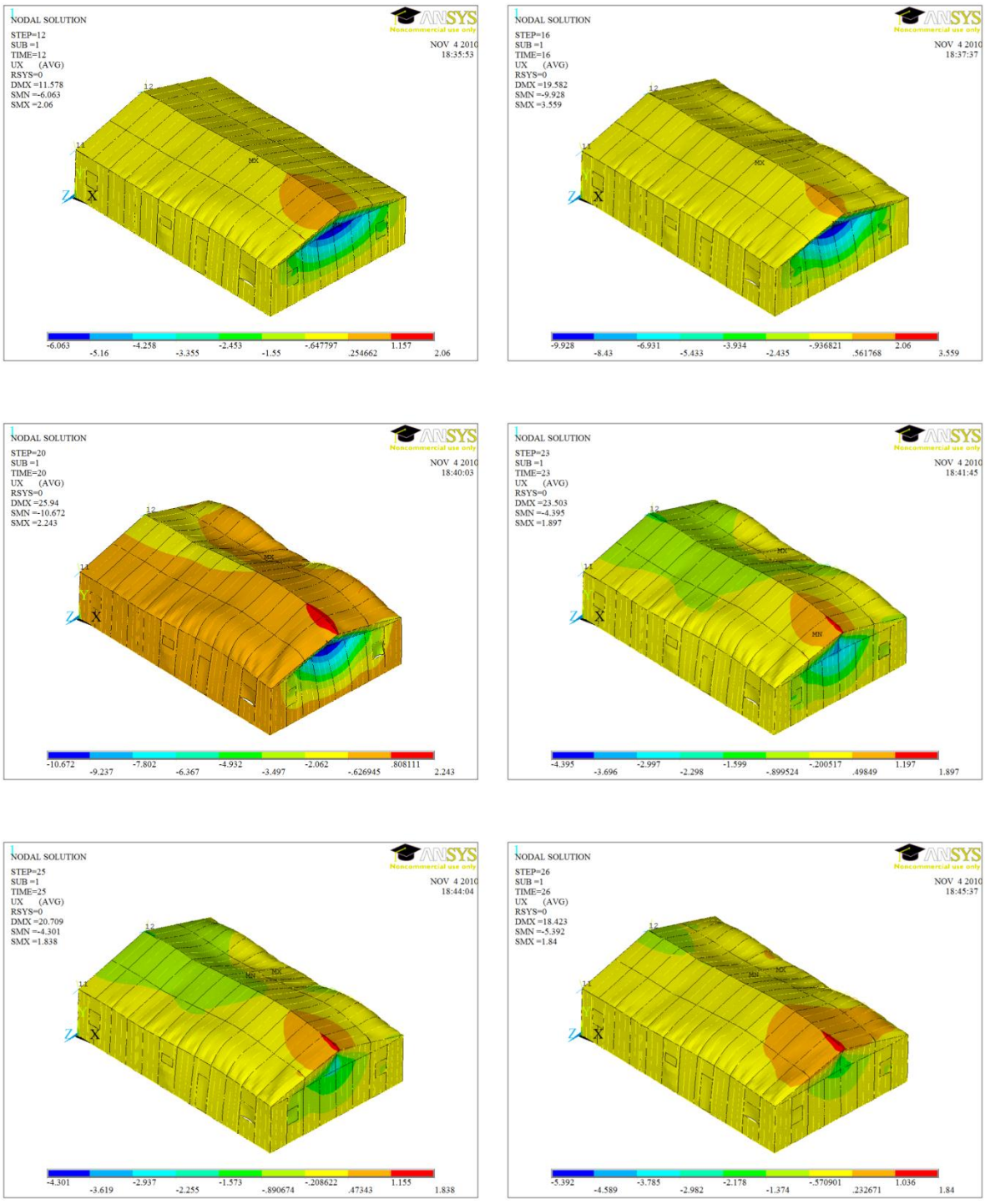

Fig. 4. Contd.. Nodal displacements in X direction for x= -1r_c, 0r_c, 1r_c, 2r_c, 3r_c, 4r_c (left to right through each row)

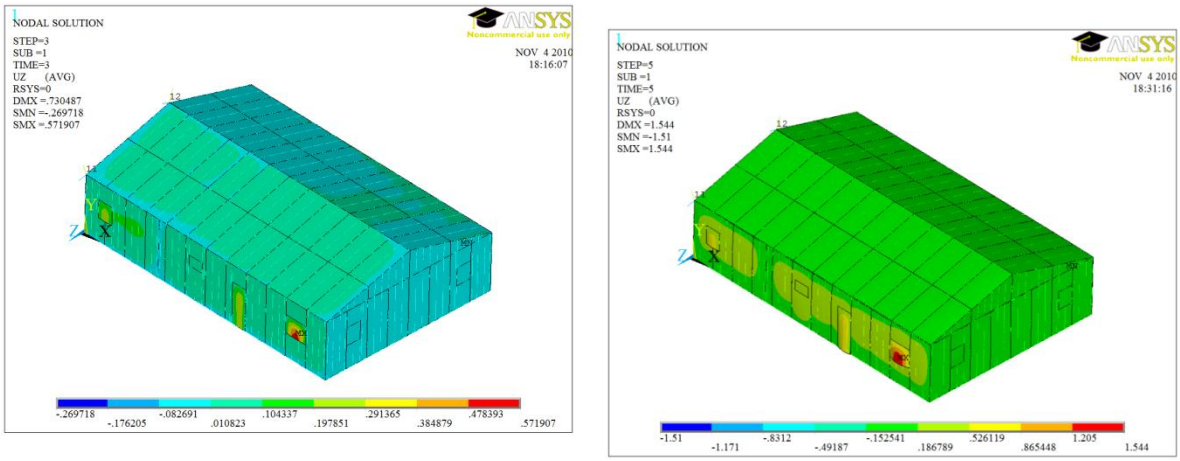

x= -4r_c x= -3r_c

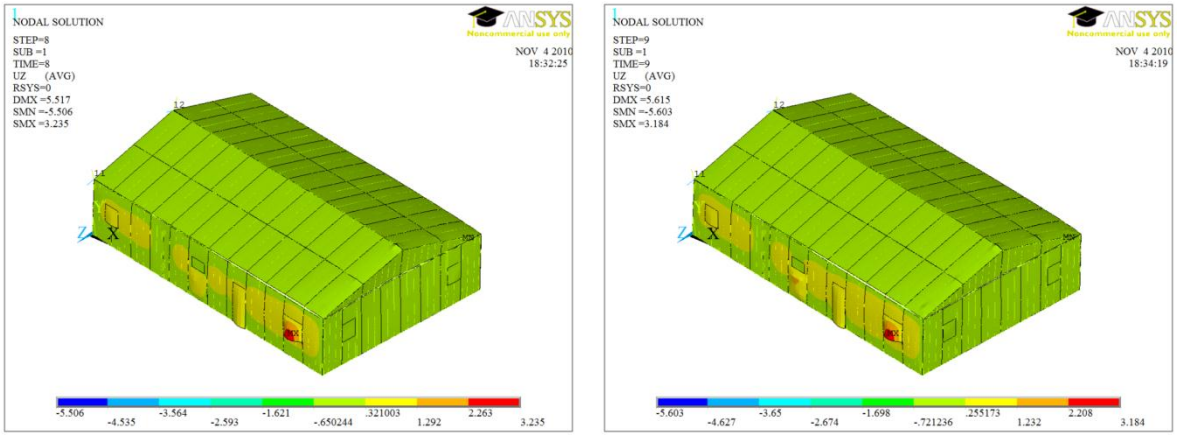

x= -2r_c x= -1.65r_c

Fig. 5. Nodal displacement in the Y direction for building faces on the +X, –Y and +Z planes for different tornado positions w.r.t. the center of the building (sealed building)

Note: Blue represents positive displacement and red represents negative displacement on the Y axis. The global Y axis equals the negative Z FE axis, Z_{FE}. The failed elements have not been removed in these plots. For better representation of failure in the figures, the scale of the deformation used for plotting has been magnified. Deflection is in inches (1 in=0.0254 m).

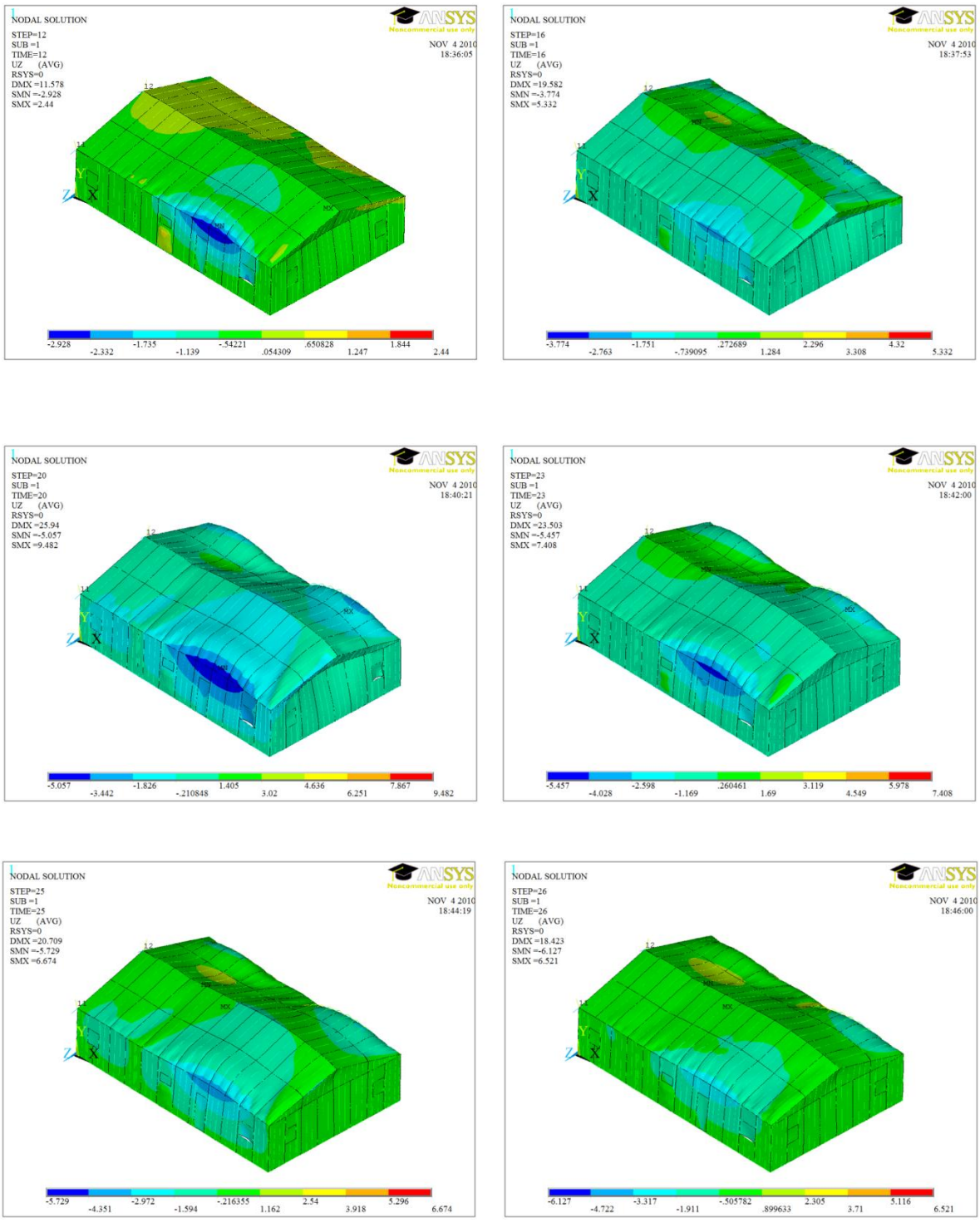

Fig. 5. Contd.. Nodal displacements in Y direction for x= -1r_c, 0r_c, 1r_c, 2r_c, 3r_c, 4r_c (left to right through each row)

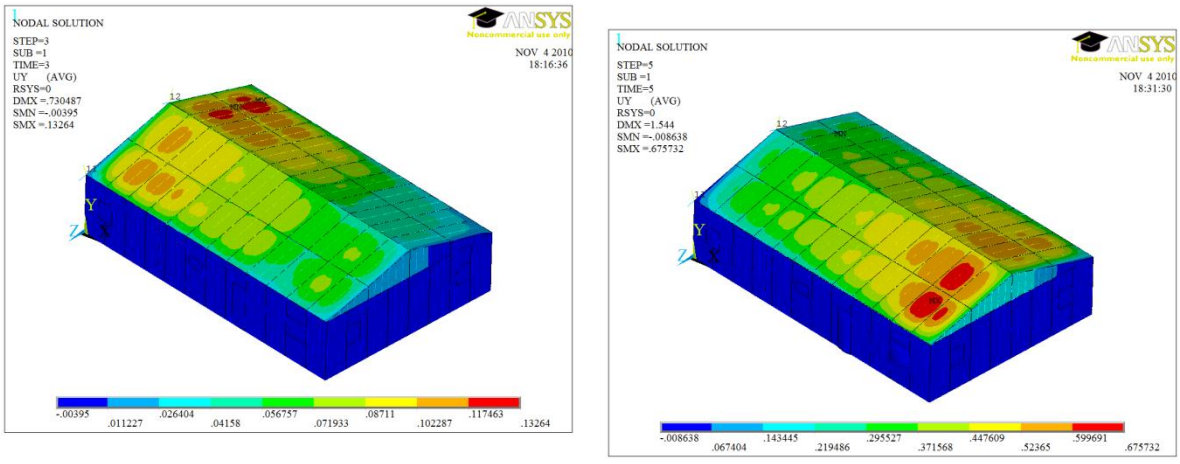

x= -4r_c x= -3r_c

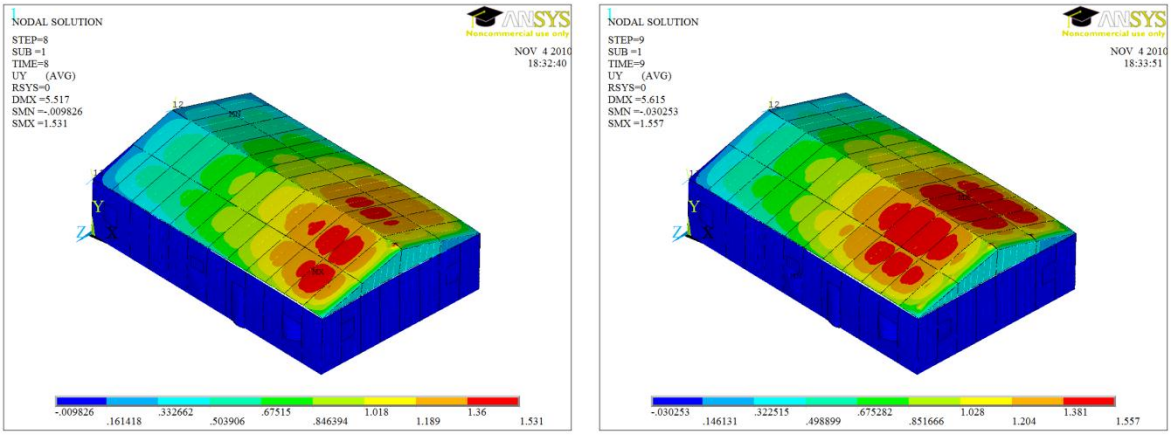

x= -2r_c x= -1.65r_c

Fig. 6. Nodal displacement in the Z direction for building faces on the +X, –Y and +Z planes for different tornado positions w.r.t. the center of the building (sealed building)

Note: Blue represents negative displacement and red represents positive displacement on the Z axis. The global Z axis equals the positive Y FE axis, Y_{FE}. The failed elements have not been removed in these plots. For better representation of failure in the figures, the scale of the deformation used for plotting has been magnified. Deflection is in inches (1 in=0.0254 m).

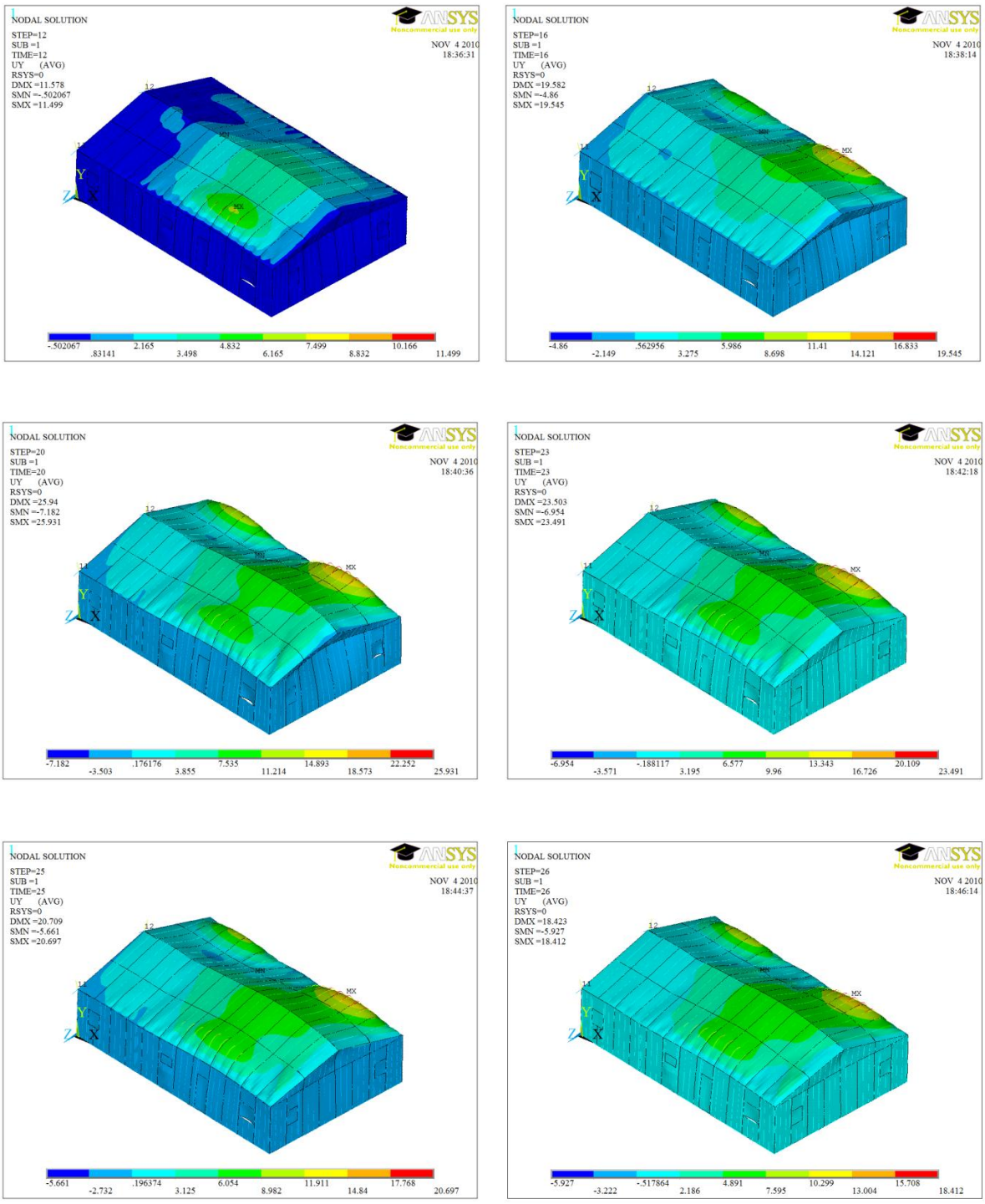

Fig. 6. Contd.. Nodal displacements in Z direction for x= -1r_c, 0r_c, 1r_c, 2r_c, 3r_c, 4r_c (left to right through each row)

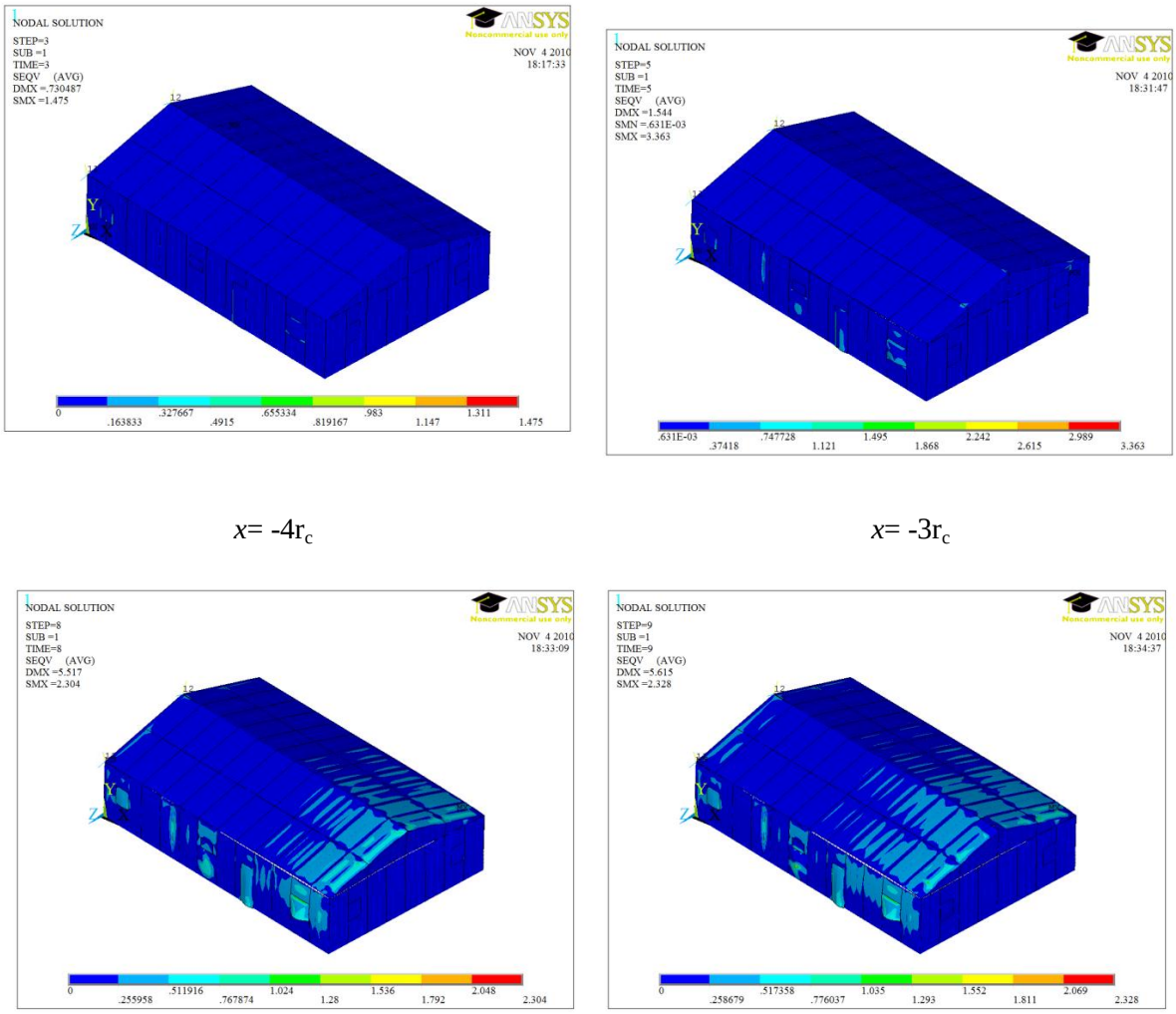

x= -4r_c x= -3r_c

x= -2r_c x= -1.65r_c

Fig. 7. Nodal Von Mises stress for building faces on the +X, –Y and +Z planes for different tornado positions w.r.t. the center of the building (sealed building)

Note: Blue represents 0 or minimum Von Mises stress and red represents positive Von Mises stress. The failed elements have not been removed in these plots. For better representation of failure in the figures, the scale of the deformation used for plotting has been magnified. Stress is in ksi (1 ksi=6.895 MPa).

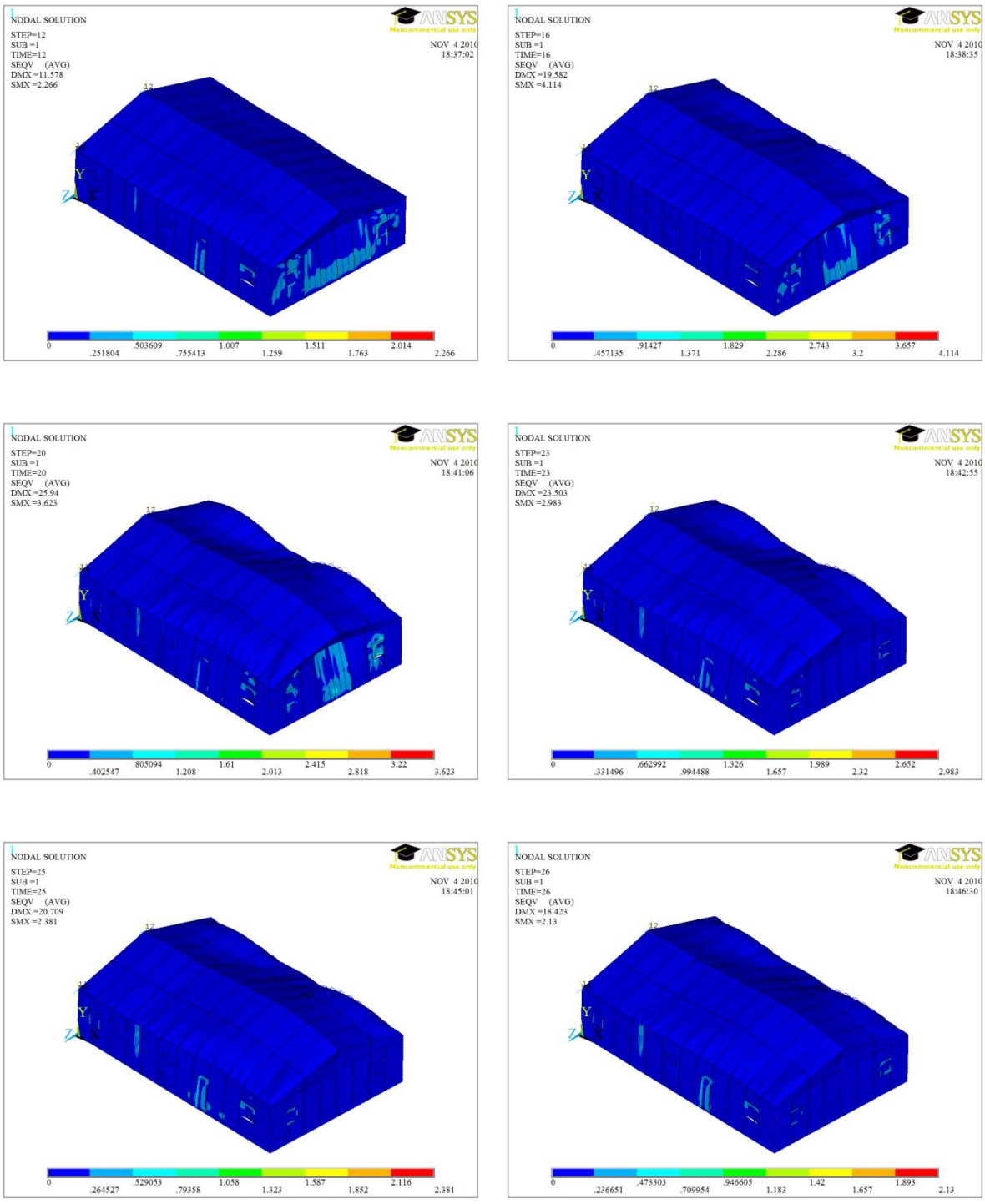

Fig. 7. Contd.. Nodal Von Mises stress x= -1r_c, 0r_c, 1r_c, 2r_c, 3r_c, 4r_c (left to right through each row)

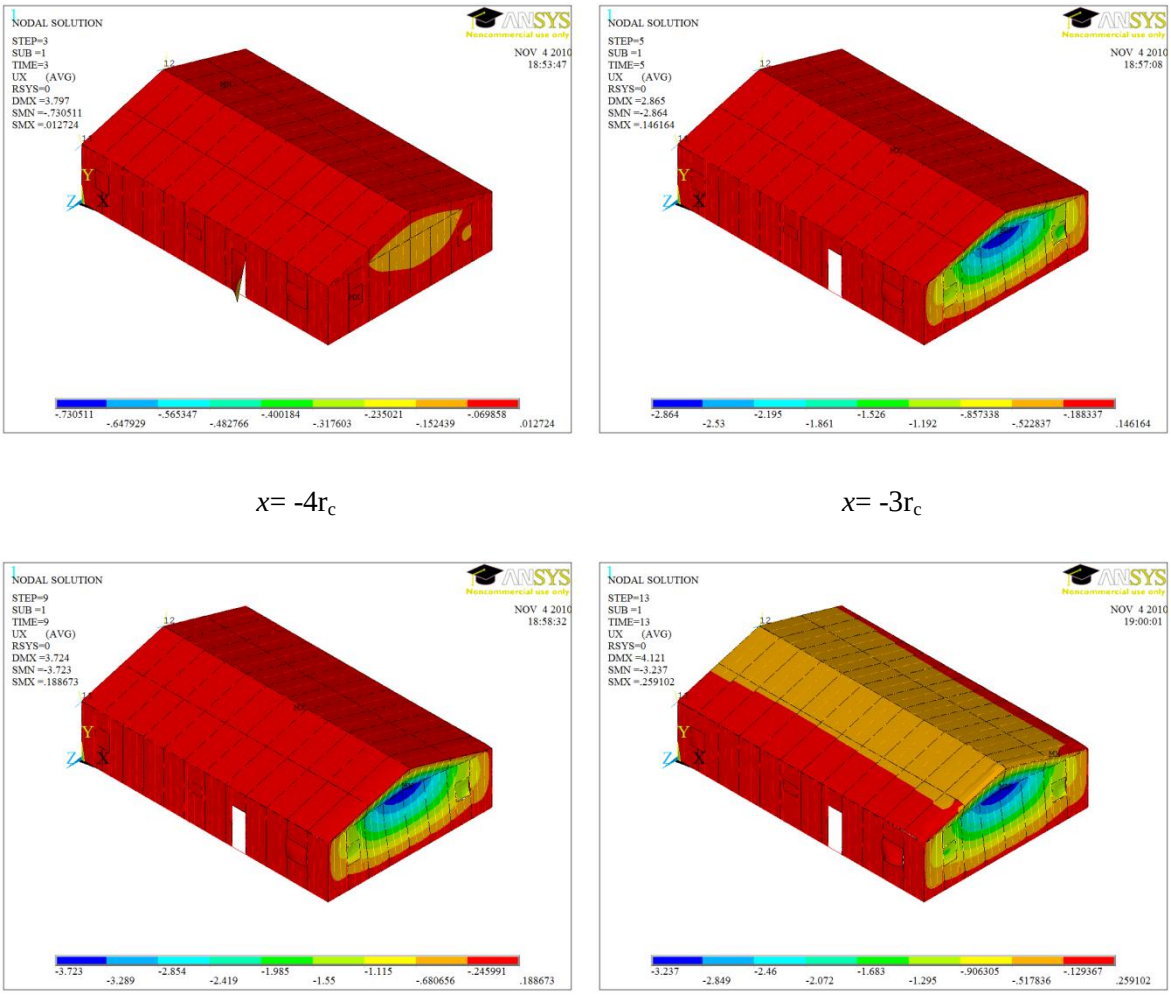

$x = -4r_c$ $x = -3r_c$

$x = -2r_c$ $x = -1r_c$

Fig. 8. Nodal displacement in the X direction for building faces on the +X, –Y and +Z planes for different tornado positions w.r.t. the center of the building (partially fixed door)

Note: Blue represents negative displacement and red represents positive displacement on the X axis. The failed elements have not been removed in these plots. For better representation of failure in the figures, the scale of the deformation used for plotting has been magnified. Deflection is in inches (1 in=0.0254 m).

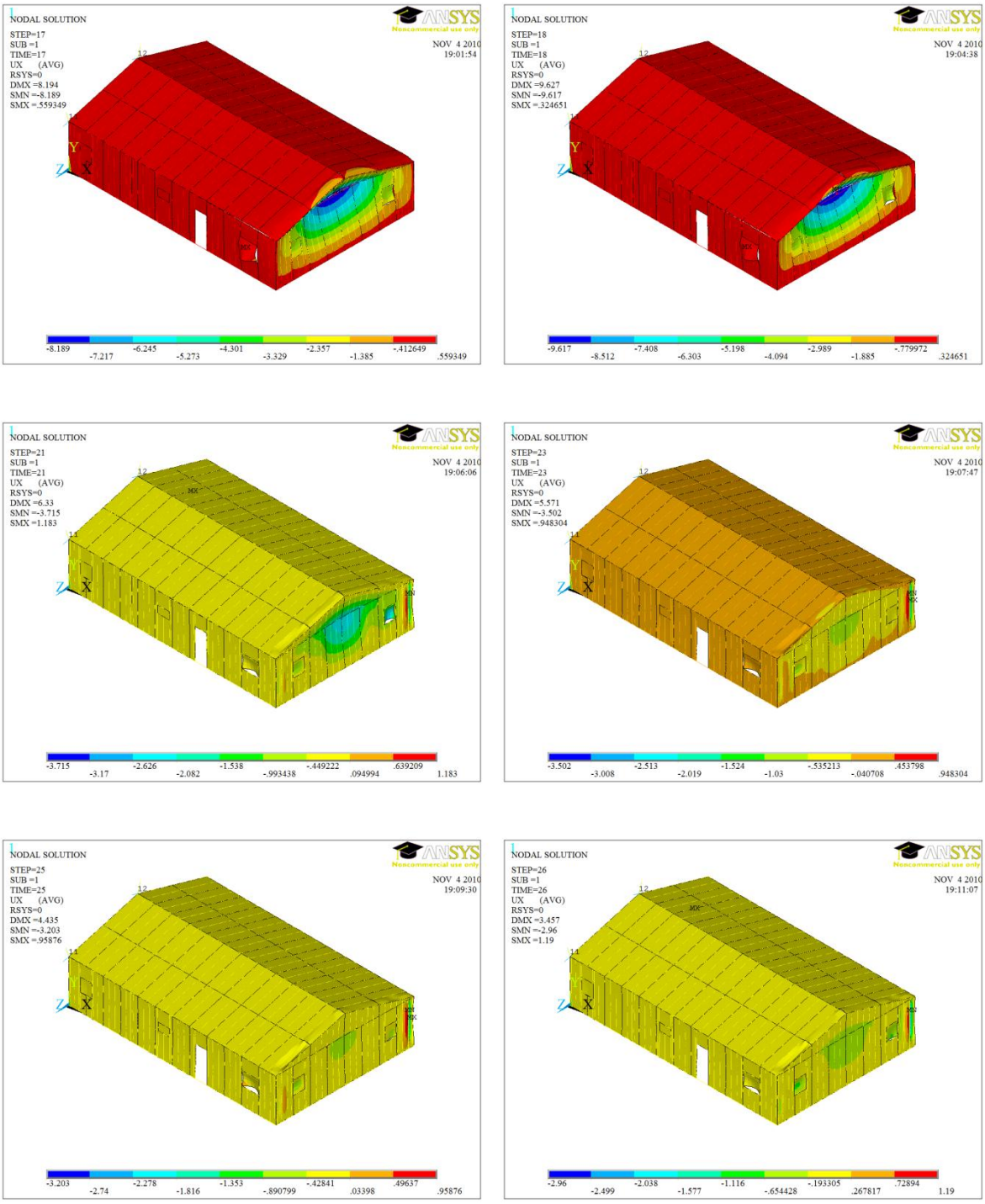

Fig. 8. Contd.. Nodal X displacement for x=0r_c, 0.25r_c, 1r_c, 2r_c, 3r_c, 4r_c (left to right through each row)

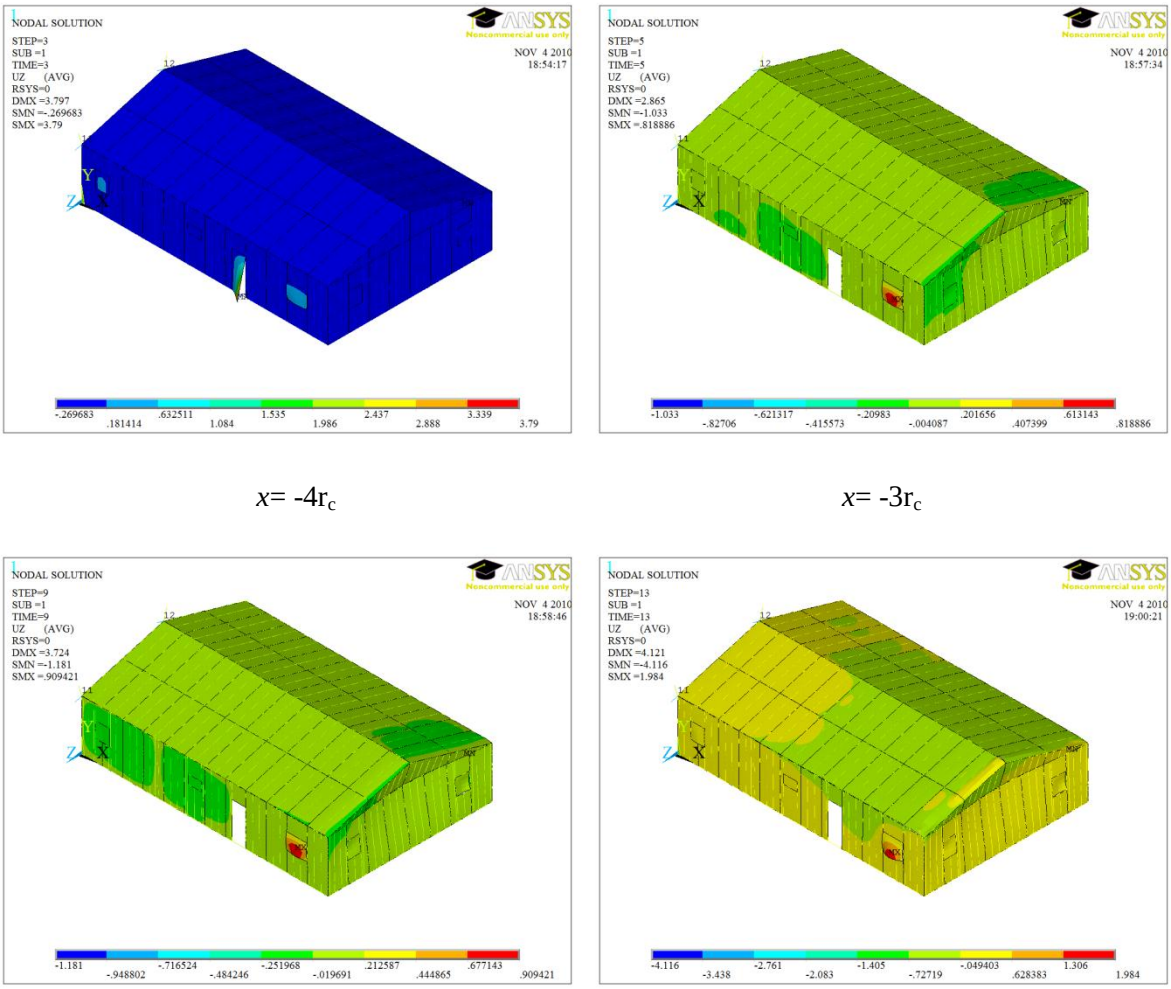

$x = -4r_c$ $x = -3r_c$

$x = -2r_c$ $x = -1r_c$

Fig. 9. Nodal displacement in the Y direction for building faces on the +X, –Y and +Z planes for different tornado positions w.r.t. the center of the building (partially fixed door)

Note: Blue represents positive displacement and red represents negative displacement on the Y axis. The global Y axis equals the negative Z FE axis, Z_{FE}. The failed elements have not been removed in these plots. For better representation of failure in the figures, the scale of the deformation used for plotting has been magnified. Deflection is in inches (1 in=0.0254 m).

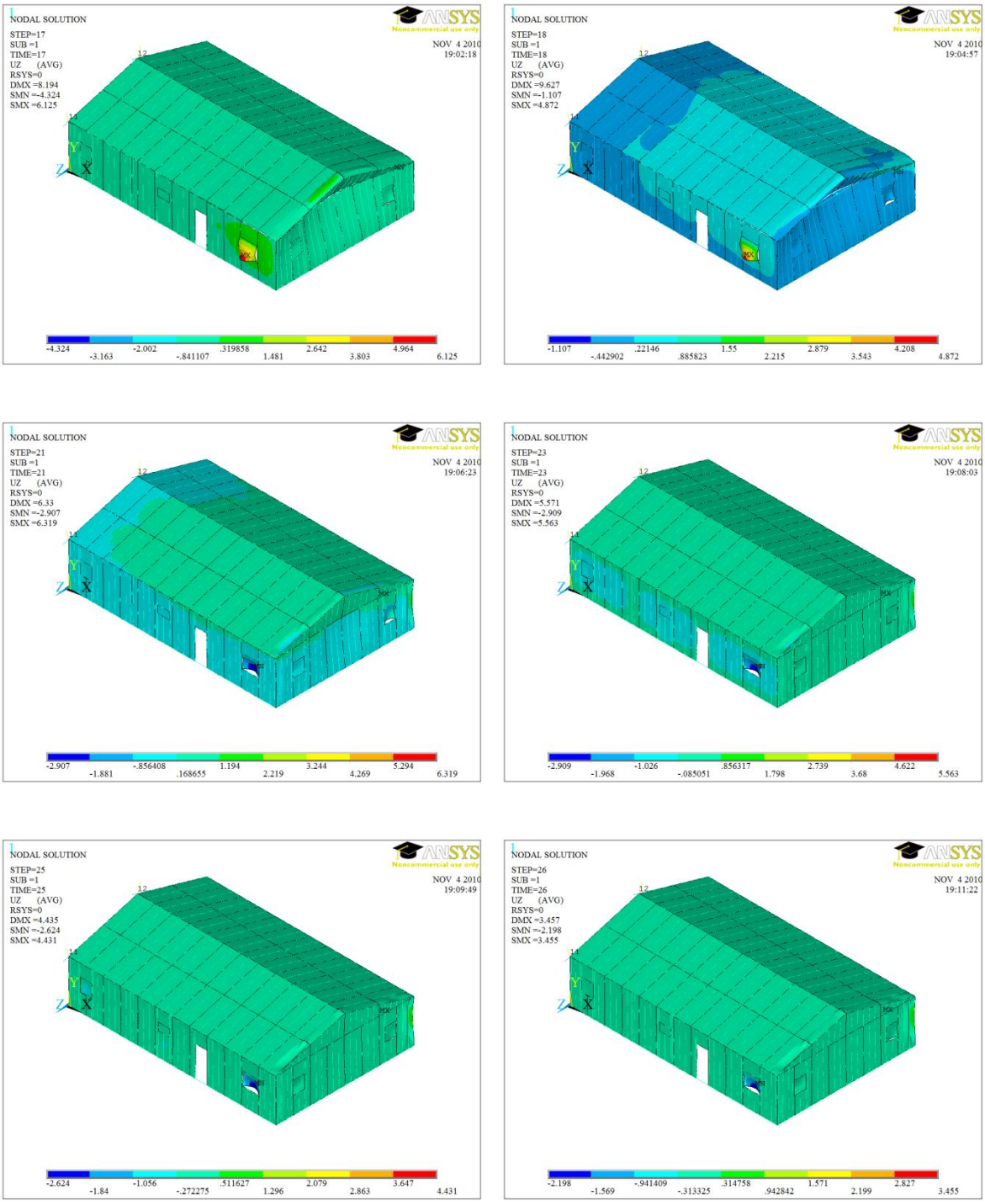

Fig. 9. Contd.. Nodal Y displacement for x=0r_c, 0.25r_c, 1r_c, 2r_c, 3r_c, 4r_c (left to right through each row)

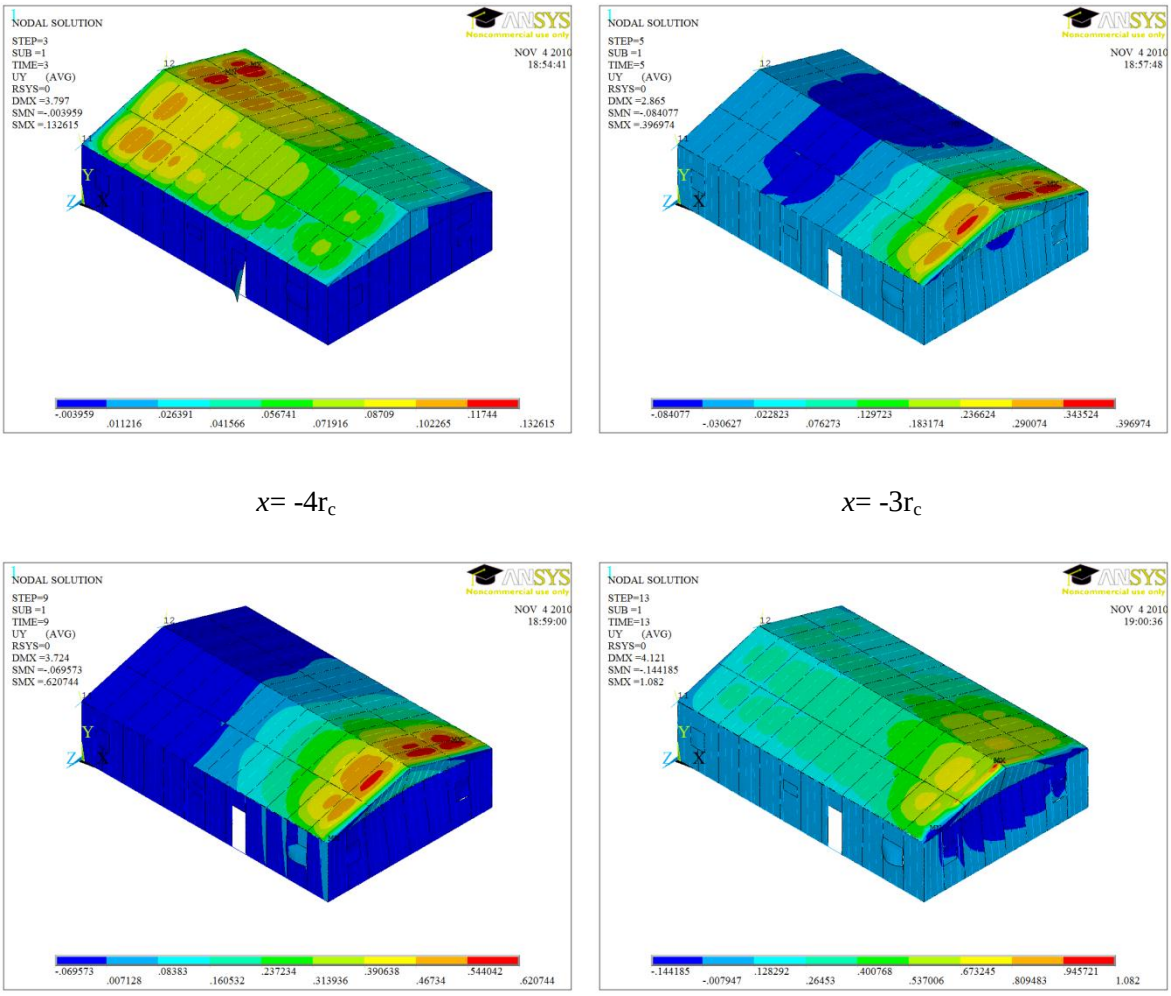

$x = -4r_c$ $x = -3r_c$

$x = -2r_c$ $x = -1r_c$

Fig. 10. Nodal displacement in the Z direction for building faces on the +X, –Y and +Z planes for different tornado positions w.r.t. the center of the building (partially fixed door)

Note: Blue represents negative displacement and red represents positive displacement on the Z axis. The global Z axis equals the positive Y FE axis, Y_{FE}. The failed elements have not been removed in these plots. For better representation of failure in the figures, the scale of the deformation used for plotting has been magnified. Deflection is in inches (1 in=0.0254 m).

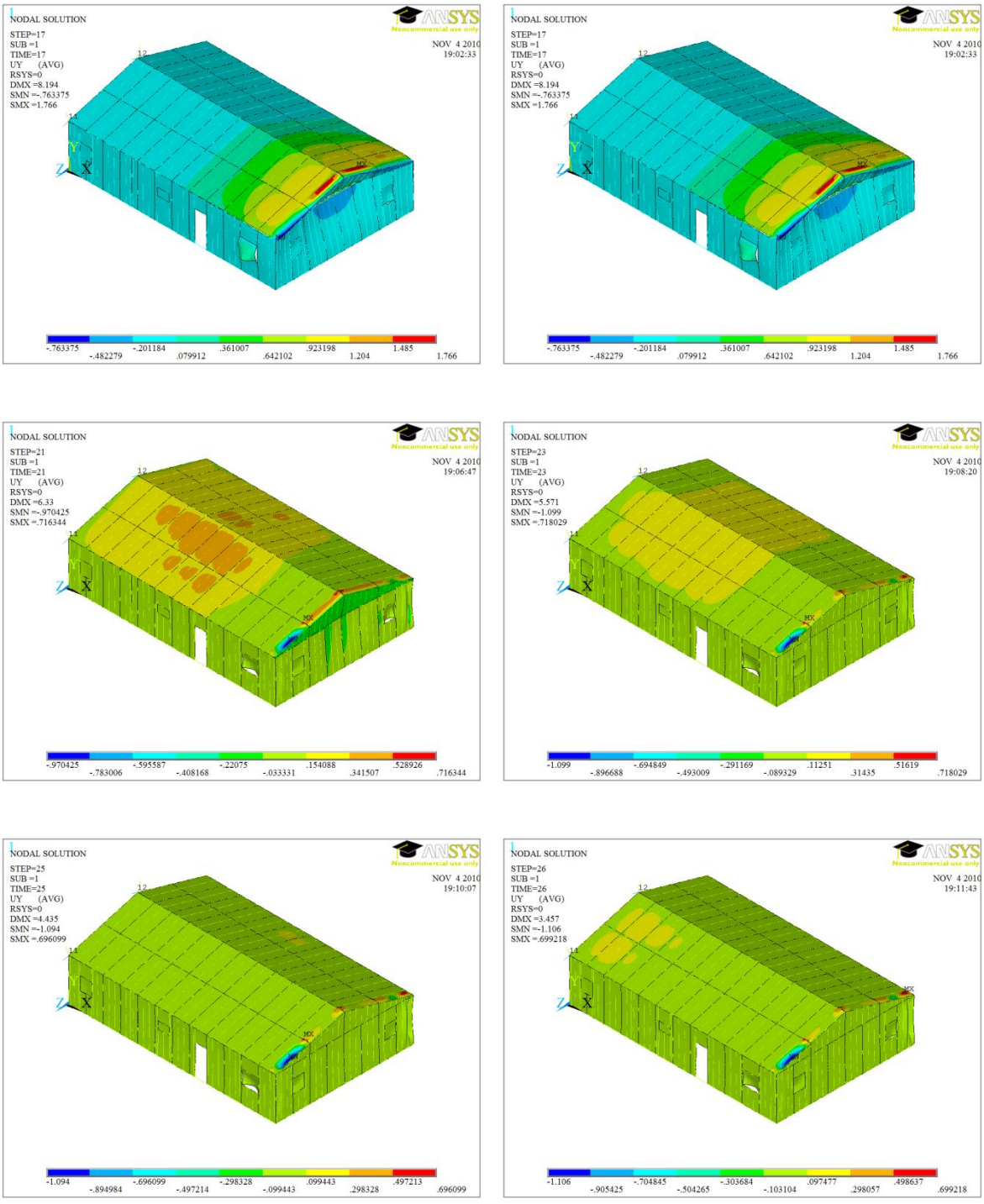

Fig. 10. Contd.. Nodal Z displacement for x=0r_c, 0.25r_c, 1r_c, 2r_c, 3r_c, 4r_c (left to right through each row)

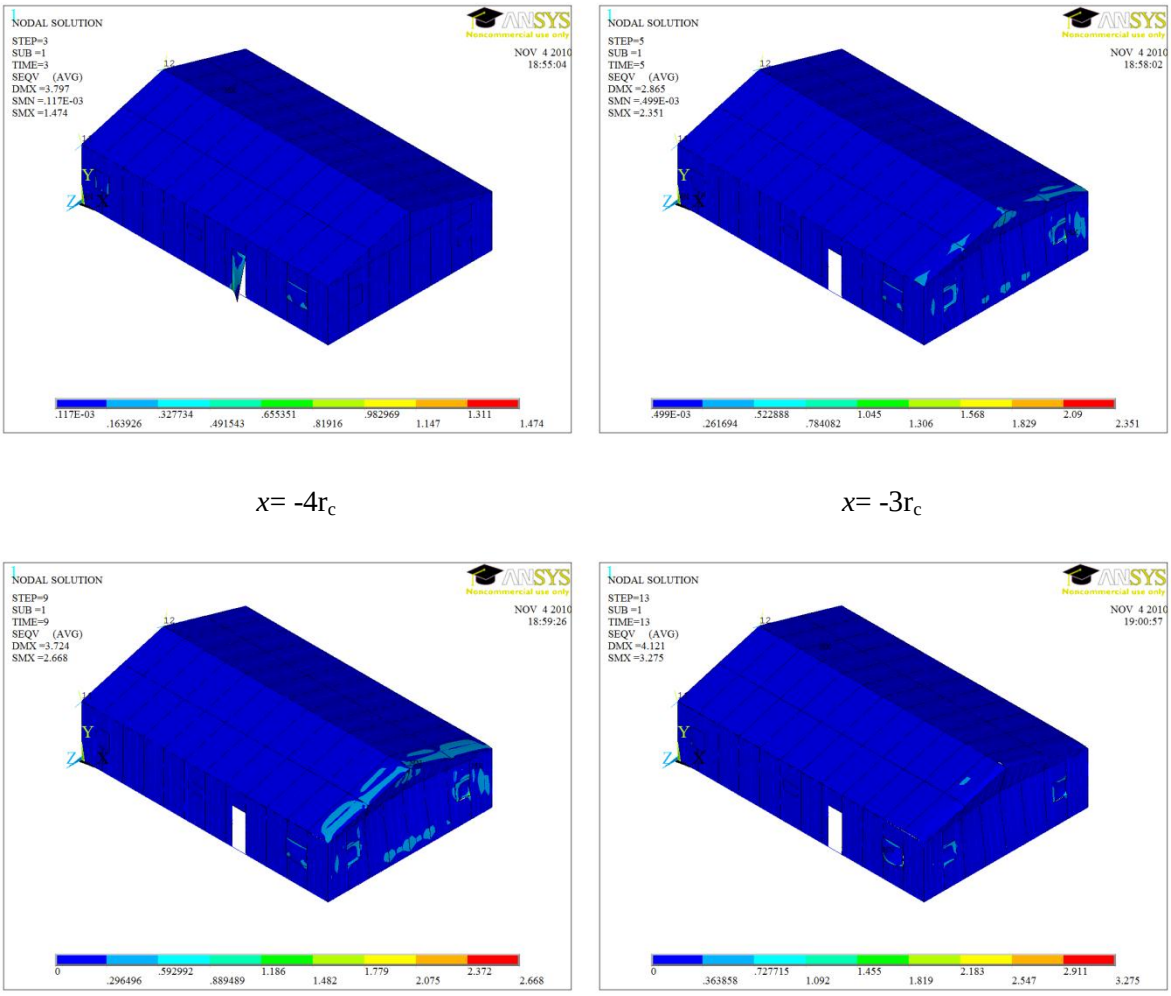

$x = -4r_c$ $x = -3r_c$

$x = -2r_c$ $x = -1r_c$

Fig. 11. Nodal Von Mises stress for building faces on the +X, –Y and +Z planes for different tornado positions w.r.t. the center of the building (partially fixed door)

Note: Blue represents 0 or minimum Von Mises stress and red represents positive Von Mises stress. The failed elements have not been removed in these plots. For better representation of failure in the figures, the scale of the deformation used for plotting has been magnified. Stress is in ksi (1 ksi=6.895 MPa).

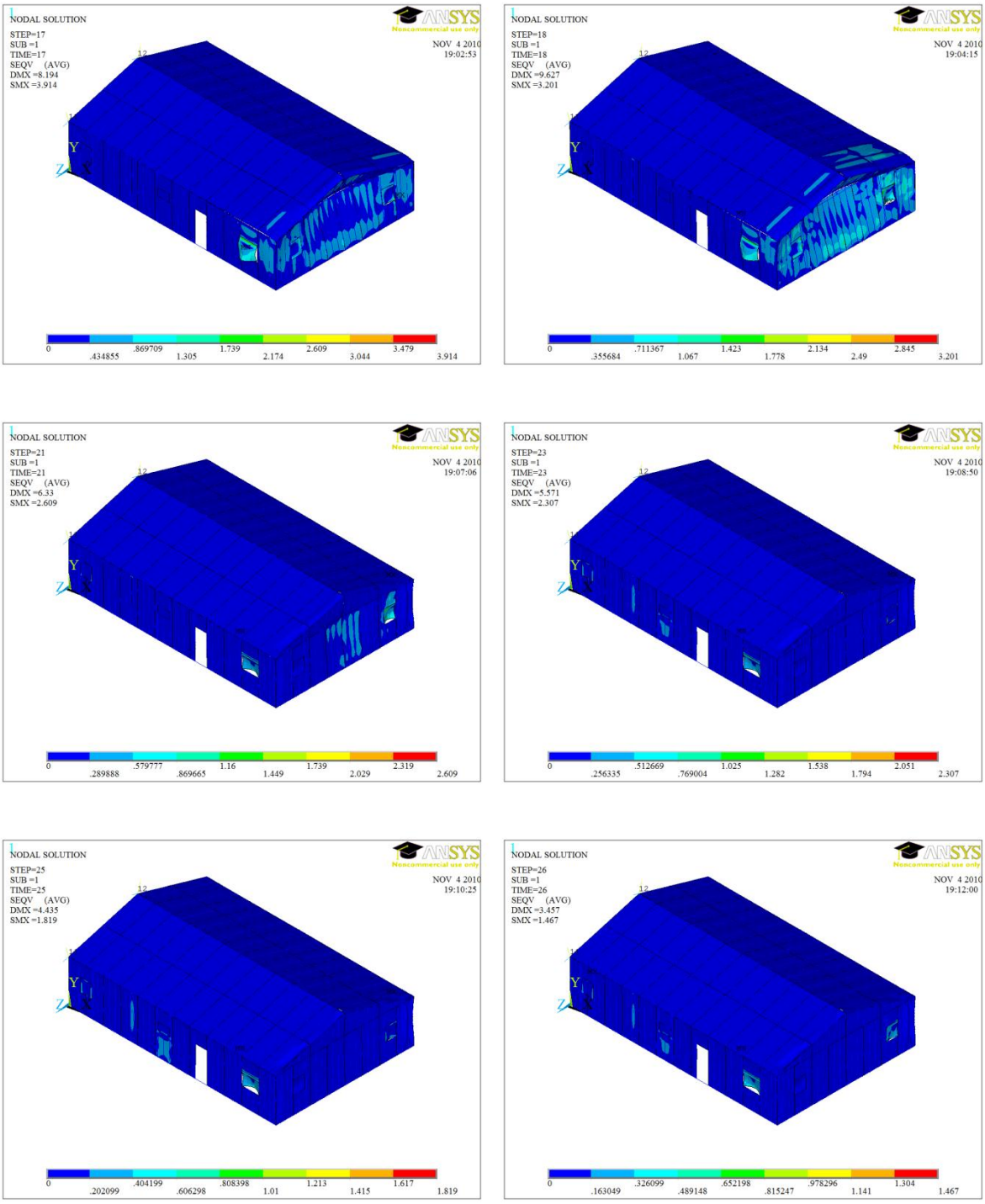

Fig. 11. Contd.. Nodal Von Mises stress for x=0r_c, 0.25r_c, 1r_c, 2r_c, 3r_c, 4r_c (left to right through each row)

CHAPTER 4

SUMMARY, CONCLUSIONS AND RECOMMENDATIONS

4.1 SUMMARY AND CONCLUSIONS OF CURRENT WORK

Experimental and numerical studies on the interaction of the wind in a translating tornado with a low-rise building were performed. The summary and conclusions made from the results are as follows.

- In the first journal paper, a methodology was developed and validated to compute the time histories of the mean force-coefficients for a low-rise building in a translating tornado, using the existing mean force-coefficients of the building in straight line winds. A tornado of swirl ratio S=1.14 and a gable-roofed low-rise building, geometrically scaled to 1:100 were used for the experimental part of this study.
- This methodology preserved the effects of tornado-building interaction and the sudden pressure drop on the outer surfaces of the building due to the tornado vortex. It is simple and can be used with ease for the design and analysis of low-rise buildings in tornados.
- This work shows that it is possible to predict the time histories of the load-coefficients of a building located at any position w.r.t. the translating tornado, from the time histories of the load-coefficients of the same building at a given position w.r.t. the translating tornado, for various building-orientations. This becomes useful when one requires the time histories of the load-coefficients at a given position for a given building-orientation but has the time histories for another position w.r.t. the translating tornado, for a few building-orientations, and wants to avoid repeated tests in a tornado simulator.
- In the second journal paper, a partially damaged one-story building, located within the damage path of the Parkersburg EF5 tornado (May 25, 2008), was chosen for analysis using FE and comparison of observed damage to those predicted in this study. The dynamic internal and external pressures on the building as the tornado

translates by the building were assessed with a geometrically scaled model (1:75) of the building placed in the ISU's Tornado/Microburst Simulator. The scaling parameters (geometric and flow parameters) for the experiments were set to resemble the example building in the Parkersburg tornado (EF5). A detailed finite element analysis of the building was performed with pressure data at a given tornado location. The damage predicted from the analysis compared well with that of the partially damaged example building seen in Parkersburg.

- The same process was repeated for tornados of intensity EF4 and EF3. The building experienced a similar damage, but with lower damage intensity under the EF4 tornado. It was subjected to minor damage (sheathing failure) but sustained the tornado of intensity EF3. This study showed that a tornado of intensity EF4 could have been sufficient to inflict the same degree of damage as seen in the partially damaged example building at Parkersburg.
- The methodology proposed here enabled accurate prediction of wind loads under the influence of a tornado for better design and construction practices. It was used to predict the stage-wise failure of the structural components of a gable-roofed timber building when hit by a tornado.
- The study provided a better understanding of the influence of dynamically varying internal pressure on the building performance during a tornado. It helped in assessing the intensity of a tornado from the observed damage state of the building.
- From the analysis, it was found that roof uplift connectors designed for resisting 90 mph straight line wind as per building code barely resist 90 mph tornado wind in a sealed building.
- A study of the influence of leakage on the wind loading on the building was performed from which it was suggested that leakage and openings could be vital in alleviating tornado induced damage.

4.2 RECOMMENDATIONS FOR FUTURE RESEARCH

Based on the research accomplishments as described above, the following recommendations are suggested.

- While predicting the time histories of force-coefficients for a low-rise building in a translating tornado using the existing mean force-coefficients of the building in straight line winds, the effects of vertical velocity can be implemented to obtain better results.
- In the work performed to predict the damage of a low-rise building under a translating tornado using FE method, it is encouraging that the effects of debris in a tornado be implemented in a similar study. The study can be performed to analyze on a group of buildings in different terrains, to see the changes in modes of failure and to improve the understanding of the EF scale.
- The performance of new and lightweight materials as different structural components and improved connections to reduce the damage intensity in a tornado can be studied.
- As there has been an improved knowledge in the influence of openings on net wind loads in a tornado, studies can be performed to optimize the internal and external geometry of the building to reduce net wind loads in a tornado.
- The effect of turbulence in the wind loads of a tornado and the sudden formation of openings need to be incorporated to capture more accurately the effects of the dynamic wind's interaction with the structure.

REFERENCES

AF&PA, 2001. Details for conventional wood frame construction, 2001. American Forest and Paper Association.

Andreasson, S., Yasumura, M., Daudeville, L., 2002. Sensitivity study of the finite element model for wood-framed shear walls, Journal of Wood Sciences, The Japan Wood Research Society, 48, 171-178.

ANSYS. Academic research 12.1, help system, ANSYS Inc.

APA, 1997. Plywood Design Specifications 1997. APA, The Engineering Wood Association.

ASTM-D1761-06, 2008. Annual book of ASTM standards 2008-standard test methods for mechanical fasteners in wood, ASTM International.

Aune, P., Mallory, M.P., 1986. Lateral load-bearing capacity of nailed joints based on the yield theory-experimental verification. United States Department of Agriculture, Research Paper FPL 470.

Chang, C.C., 1971. Tornado wind effects on buildings and structures with laboratory simulation. Proceedings of the Third International Conference on Wind Effects on Buildings and Structures, Tokyo, 213–240.

Chow, P., McNatt, J.D., Lambrechts, S.J., Gertner, G.Z., 1988. Direct withdrawal and head pull-through performance of nails and staples in structural wood-based panel materials, Forest Products Journal, 38, 19-25.

Church, C.R., Snow, J.T., Baker, G.L., Agee, E.M., 1979. Characteristics of tornado like vortices as a function of swirl ratio: A laboratory investigation, Journal of the Atmospheric Sciences 36, 1755–1776.

Collins, M., Kasal, B., Paevere, P.J., Foliente, G.C., 2005. Three-dimensional model of light frame wood buildings I: model description. Journal of Structural Engineering 131, 676-683.

Collins, M., Kasal, B., Paevere, P.J., Foliente, G.C., 2005. Three-dimensional model of light frame wood buildings II: experimental investigation and validation of analytical model. Journal of Structural Engineering 131, 684-692.

Dutta, P.K., Ghosh, A.K., Agarwal, B.L., 2002. Dynamic response of structures subjected to tornado loads by FEM. Journal of Wind Engineering and Industrial Aerodynamics 10, 55-69.

Fiedler, B.H., 1993. Numerical simulation of axisymmetric tornadogenesis in forced convection. In: Church CR, et al., editors. The tornado: Its structure, dynamics, prediction, and hazards, Geophysical monograph, American Geophysical Union, 79.

Foliente, G.C., 1995. Hysterisis modeling of wood joint and structural systems, Journal of Structural Engineering, 121, 1013-1022.

Haan, F.L., Balaramudu, V.K., Sarkar, P.P., 2010. Tornado-induced wind loads on a low-rise building. American Society of Civil Engineers, Journal of the Structural Division 136, 106–116.

Haan, F.L., Sarkar, P.P., Gallus, W.A., 2008. Design, construction and performance of a large tornado simulator for wind engineering applications. Engineering Structures 30, 1146-1159.

He, M., Lam, M., Foschi, R.O., 2001. Modeling three-dimensional timber light-frame buildings, Journal of Structural Engineering, 127, 901-913.

Herzog, B.,Yeh, B. Nail withdrawal and pull-through strength of structural –use panels, APA – The Engineered Wood Association.

Holmes, J.D., 1978. Mean and fluctuating internal pressures induced by wind, Wind Engineering Report 5/78. Department of Civil and Systems Engineering, James Cook University of North Queensland, Australia.

IBC, 2006. 2006 International Building Code. International Code Council, Inc.

Jischke, Light, 1983. Laboratory simulations of tornadic wind loads on a rectangular model structures. Journal of Wind Engineering and Industrial Aerodynamics 13, 371–382.

Judd, J.P., Fonseca, F.S., 2005. Analytical model for sheathing-to-framing connections in wood shear walls and dia-phragms. Journal of Structural Engineering 131, 345-352.

Kasal, B., Leichti, R. J., Itani, R.Y., 1994. Nonlinear finite-element model of complete light-frame wood structures. Journal of Structural Engineering 120, 110-119.

Kuai, L. Haan, F.L., Gallus, W.A., Sarkar, P.P., 2008. CFD simulations of the flow field of a laboratory-simulated tornado for parameter sensitivity studies and comparison with field measurements. Wind and Structures 11, 75-96.

Kumar, N., 2008. Stress analysis of wood-framed low-rise buildings under wind loads due to tornados. Master of Science thesis, Iowa State University.

Kuo, H.L., 1966. On the dynamics of convective atmospheric vortices. Journal of Atmospheric Sciences 23, 25-42.

Kuo, H.L., 1971. Axisymmetric flows in the boundary layer of a maintained vortex. Journal of Atmospheric Sciences 28, 20-41.

Mehta, K.C., Mcdonald, J.R., Minor, J., 1976. Tornadic loads on structures. Proceedings of the Second USA–Japan Research Seminar on Wind Effects on Structures, Tokyo, Japan, 15–25.

Oh, J.H., Kopp, G.A., Inculet, D.R., 2007. The UWO contribution to the NIST aerodynamic database for wind loads on low buildings: Part 3. Internal pressures. Journal of Wind Engineering and Industrial Aerodynamics 95, 755-779.

Paevere, P.J., Kasal, B., Foliente, G.C., 2003. Load-sharing and re-distribution in a one-story wood frame building. Journal of Structural Engineering 129, 1275–1284.

Sarkar, P.P., Kikitsu, H., 2008. Damage survey report on Parkersburg and New Hartford, Iowa, EF5-tornado of May 25, 2008.

Savory, E., Parke, G.A.R., Zeinoddini, M., Toy, N., Disney, P., 2001. Modeling of tornado and microburst-induced wind loading and failure of a lattice transmission tower. Engineering Structures 23, 365-375.

Sengupta, A., Haan, F.L., Sarkar, P.P., Balaramudu, V., 2008. Transient loads on buildings in microburst and tornado winds. Journal of Wind Engineering and Industrial Aerodynamics 96, 2173-2178.

Sparks, P.R., Hessig, M.L., Murden, J.A., Sill, B.L., 1988. On the failure of single storied wood framed houses in severe storms. Journal of Wind Engineering and Industrial Aerodynamics 29, 245–252.

Ward, N.B., 1972. The exploration of certain features of tornado dynamics using a laboratory model. Journal of the Atmospheric Sciences 29, 1194–204.

Wen, Y.K., 1975. Dynamic Tornadic wind loads on tall buildings. American Society of Civil Engineers, Journal of the Structural Division 101, 169–185.

Wen, Y.K., Ang, A.H.S., 1975. Tornado risk and wind effects on structures. Proceedings of the Fourth International Conference on Wind Effects on Buildings, Heathrow, pp. 63– 74.

WFCM, 2006. Guide to wood construction in high wind areas for one- and two- family dwellings. American Forest and Paper Association.

Matweb, 2010. http://www.matweb.com, September 14, 2010.